



**HAL**  
open science

# Recent progress on chemical modification of cellulose nanocrystal (CNC) and its application in nanocomposite films and membranes-A comprehensive review

Chaimaa Gomri, Marc Cretin, M. Semsarilar

## ► To cite this version:

Chaimaa Gomri, Marc Cretin, M. Semsarilar. Recent progress on chemical modification of cellulose nanocrystal (CNC) and its application in nanocomposite films and membranes-A comprehensive review. *Carbohydrate Polymers*, 2022, 294, pp.119790. 10.1016/j.carbpol.2022.119790 . hal-04065841

**HAL Id: hal-04065841**

**<https://hal.umontpellier.fr/hal-04065841v1>**

Submitted on 13 Oct 2023

**HAL** is a multi-disciplinary open access archive for the deposit and dissemination of scientific research documents, whether they are published or not. The documents may come from teaching and research institutions in France or abroad, or from public or private research centers.

L'archive ouverte pluridisciplinaire **HAL**, est destinée au dépôt et à la diffusion de documents scientifiques de niveau recherche, publiés ou non, émanant des établissements d'enseignement et de recherche français ou étrangers, des laboratoires publics ou privés.

# 1 Recent progress on chemical modification of Cellulose 2 Nanocrystal (CNC) and its application in nanocomposite 3 films and membranes- A comprehensive review

4 Chaimaa Gomri <sup>a</sup>, Marc Cretin<sup>b</sup>, Mona Semsarilar <sup>c\*</sup>

5 <sup>a</sup> Institut Européen des Membranes, Montpellier, France, [chaimaa.gomri@umontpellier.fr](mailto:chaimaa.gomri@umontpellier.fr)

6 <sup>b</sup> Institut Européen des Membranes, Montpellier, France, [marc.cretin@umontpellier.fr](mailto:marc.cretin@umontpellier.fr)

7 <sup>c</sup> Institut Européen des Membranes, Montpellier, France, [mona.semsarilar@umontpellier.fr](mailto:mona.semsarilar@umontpellier.fr)

8

9

10

## 11 Abstract

12 Cellulose nanocrystal (CNC) has recently gained much attention due to its unique properties such as abundancy,  
13 biodegradability, high strength, large surface area, functional ability, template structure, and sustainability. To  
14 broaden its application and enhance its compatibility with other materials, CNC can be modified via different  
15 methods. The modification is based on introducing new functions, including esterification, silylation, carbamation,  
16 polymerization, and so on. The application can concern many fields, such as polymer reinforcement, packaging,  
17 water treatment, textiles, biosensors, etc. Herein, we summarize the main approaches employed for the chemical  
18 modification and the use of the modified CNC material in the preparation of nanocomposite films and membranes,  
19 along with some emerging applications.

## 20 Keywords

21 Cellulose nanocrystal (CNC); self-assembly; chemical modification; membrane; film; nanocomposite.

## 22 Content

---

23	1. Introduction.....	3
24	2. Cellulose origin, structure, and its property to form film.....	4
25	3. Chemical modification of cellulose nanocrystal.....	7
26	3.1. Graft polymerization.....	7
27	3.1.1. Atom transfer radical polymerization (ATRP).....	8
28	3.1.2. Reversible addition-fragmentation chain-transfer (RAFT).....	9

29	3.1.3.	Ring-opening polymerization (ROP).....	9
30	3.1.4.	Nitroxide-mediated polymerization (NMP).....	14
31	3.1.5.	Free-radical polymerization (FRP).....	14
32	3.2.	Grafting small molecule.....	14
33	3.2.1.	Click chemistry.....	14
34	3.2.2.	Silylation.....	15
35	3.2.3.	Esterification.....	15
36	4.	Nanocomposite film and membrane-based on cellulose nanocrystal.....	17
37	4.1.	Preparation of cellulose nanocrystal composite film and membrane.....	17
38	4.2.	Application of cellulose nanocrystal composite membrane and film.....	19
39	4.2.1.	Conductive materials.....	19
40	4.2.2.	Water treatment.....	20
41	4.2.3.	Packaging.....	23
42	4.2.4.	Biomedical.....	23
43	5.	Summary.....	24
44		Reference.....	24

## 45 **1. Introduction**

46 According to the 2019 UN report, the world population is growing at an annual rate of 1.1%, which predicts a  
47 global population of 8.5 billion in 2030, instead of the 7.7 billion recorded in mid-2019 (ONU, 2019). Admittedly,  
48 the growth rate has been decreasing since 1950. However, it is still accompanied by strong demand for food and  
49 increased exploitation of natural resources, which contribute to sizeable environmental stress and pollution  
50 (Okada, 2002)(Sudhakar et al., 2018).

51 Thus, synthetic polymers are used extensively to meet humanity's needs and ensure a more convenient way of life.  
52 These polymers often present many risks; they are persistent, hardly degradable, and their degradation by-products  
53 are often toxic. Hence the use of degradable polymers, especially biodegradable ones, is encouraged.  
54 Biodegradable polymers are defined as polymers that, in the presence of microorganisms in a natural environment,  
55 degrade into carbon dioxide and water without generating toxic by-products (Okada, 2002).

56 Biodegradable polymers are classified into three main categories (1) polyesters produced by microorganisms, (2)  
57 natural polysaccharides and other biopolymers, and (3) synthetic polymers, in particular aliphatic polyesters.  
58 Polysaccharide materials get a growing interest due to their abundance, non-toxicity, and biodegradability, which  
59 make them a good replacement for petroleum-based polymers(Garcia-Valdez et al., 2018); not only this, but they  
60 present physicochemical properties that favor their use in several other fields (Fang et al., 2019a).

61 Cellulose belongs to this family of polysaccharides; it is the most abundant biopolymer on earth, with an annual  
62 production estimated between  $10^{11}$ - $10^{12}$  tons (Nechyporchuk et al., 2016). It is used in several fields with the

63 following distribution: 28% in materials sciences, 17% in engineering, 16% in chemistry, 11% in chemical  
64 engineering, 8% in physics and astronomy, 5% in biochemistry, genetics, and molecular biology, 4% in  
65 environmental science, 3% in agriculture and biological sciences, 3% in medicine, 3% in energy, 1% in  
66 immunology and microbiology and 1% in pharmacology, toxicology, and pharmaceuticals (Mohamed et al., 2017).  
67 Cellulose can originate from wood, flax, cotton, and algae in the form of microfibrils. Mechanical and chemical  
68 treatment of these microfibrils allows for obtaining cellulose nanofibrils (CNF) and cellulose nanocrystal (CNC)  
69 (Hamad, 2002). Cellulose can also originate from bacteria and has a more crystalline structure than cellulose  
70 extracted from plants.

71 This review is dedicated to cellulose nanocrystal (CNC) specifically. The first part concerns the origin, structure  
72 of cellulose, and its ability to self-assemble and form films. The second part emphasizes the main chemical  
73 modification of CNC surfaces applied during the last decade. In contrast, the last part gathers the techniques  
74 applied to develop composite membrane and film based on CNC and their possible applications.

## 75 **2. Cellulose origin, structure, and its property to form films**

76 Natural cellulose is originated from plants through the disintegration of the microfibrils that form the cell wall  
77 (Figure 1) (Mohamed et al., 2017) (Gopakumar et al., 2018) (Dong et al., 2021); extraction can be made by  
78 chemical or mechanical treatment [14][13] and lead to two types of cellulose, cellulose nanofibrils (CNF) and  
79 cellulose nanocrystals (CNC). This approach is known as top-down biosynthesis. CNF consists of two regions, an  
80 ordered region, in other words, a crystalline region that confers high resistance to cellulose, and an amorphous  
81 region which contributes to the flexibility of the material (Phanthong et al., 2018). CNF is characterized by a  
82 diameter between 1-100 nm and a length between 500-2000 nm. When subjected to acid hydrolysis, cellulose  
83 nanofibrils undergo transverse cleavage along amorphous regions because they have a lower density due to their  
84 random orientation, resulting in the formation of cellulose nanocrystals (CNC) (Gopakumar et al., 2018)  
85 (Mohamed et al., 2017). Their dimensions depend on the starting material, their diameter varies between 2-20 nm  
86 (Sharma et al., 2020), and their length is between 100-500 nm (Gopakumar et al., 2018).

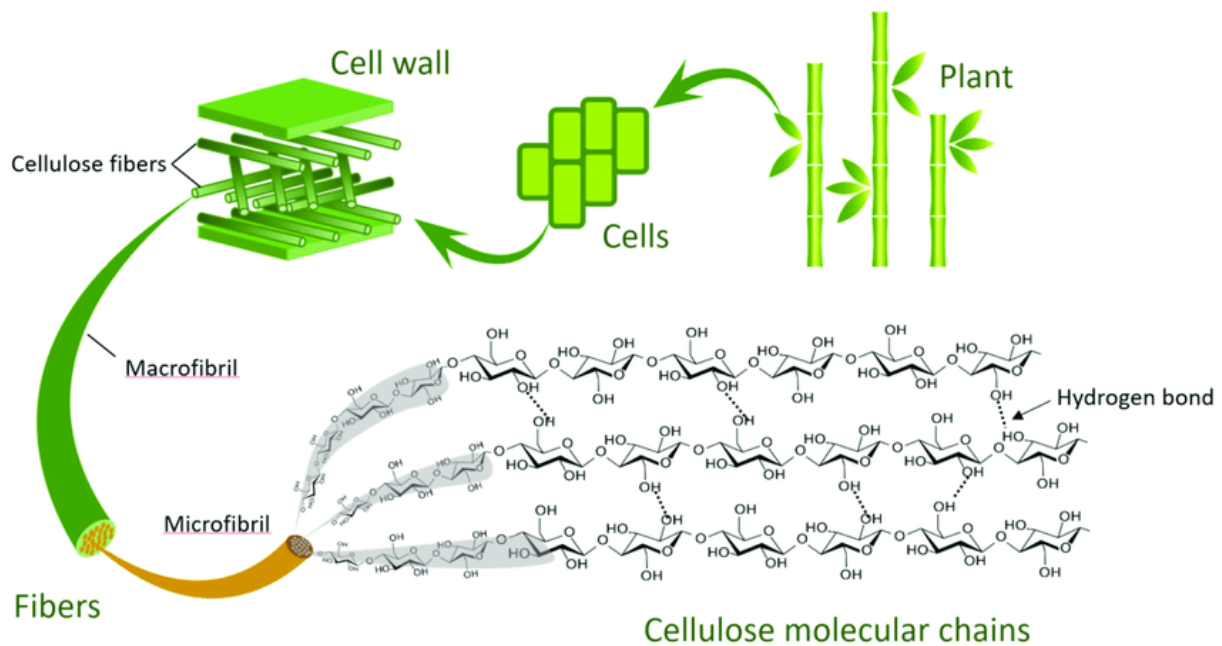
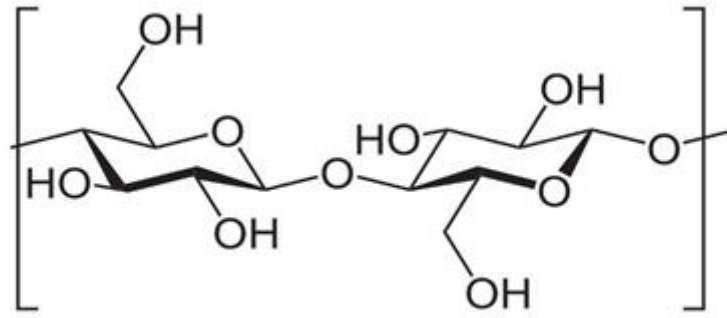


**Figure 1. Illustration of the origin of natural cellulose** (Han, 2019).

Nanocellulose can also be obtained from bottom-up biosynthesis using bacteria (Bwatanglang et al., 2020). It is produced through the pores of bacteria membranes, so *Gluconacetobacter* is the species with the highest production ability (Belaustegui et al., 2020). There are other species such as *Acinetobacter xylinum* through (Sharma et al., 2020), *Rhizobium*, *Agrobacterium*, *Sarcina* and *Alcaligenes* (Belaustegui et al., 2020). Bacterial cellulose has the form of twisting ribbons with a diameter between 20-100 nm and length in micron order (Phanthong et al., 2018). It has the same structure as the cellulose extracted from the plant wall but presents higher purity and crystallinity (Revin et al., 2018).

The formula of cellulose is  $(C_6H_{10}O_5)_n$ , with  $n$  being the degree of polymerization that depends on the source of the cellulose and the method of isolation and purification [6]. It is composed of  $\beta$ -D-glucopyranose units linked together by  $\beta$ - (1,4) -glycosidic bonds (Arfin, 2020); each unit has 3 hydroxyl groups, a primary hydroxyl group on the C6, and two hydroxyl groups secondary on C2 and C3, presenting reactive sites that allow modification of cellulose (Fleet et al., 2008) (figure 2). The reactivity of these sites is governed by factors depending on the steric effects related to the supramolecular structure of cellulose and its isomerization. The C6 primary alcohol is ten times more reactive than the C2 and C3 secondary alcohols, thanks to the free rotation around the C5 and C6 bond. (Garcia-Valdez et al., 2018). These hydroxyl groups allow the formation of inter and intramolecular hydrogen bonds (Chu et al., 2020)(Kausar, 2020). These bonds allow the formation of a solid network giving cellulose a fibrillated structure, high resistance, and insolubility in water and most organic solvents (Phanthong et al., 2018).



106

107

**Figure 2. Cellobiose unit composed of two  $\beta$ -D-glucopyranose units.**

108

CNC suspension behaves as a cholesteric crystalline liquid; this phase can be preserved after evaporation of the solvent, which leads to a well-structured iridescent film (Frka-Petesic et al., 2017). Factors such as the technique of extraction and concentration of the suspension have a direct impact on the self-assembly. CNC extracted using sulfuric acid exhibits a stable suspension due to sulfate groups negatively charged attached to the surface (Tran et al., 2020); this stability is a prerequisite to having self-assembly for cases where CNC is isolated by using phosphoric acid or hydrochloric acid, CNC will not be enough charged and will tend to flocculate which impacts the self-assembly negatively (Parker et al., 2018).

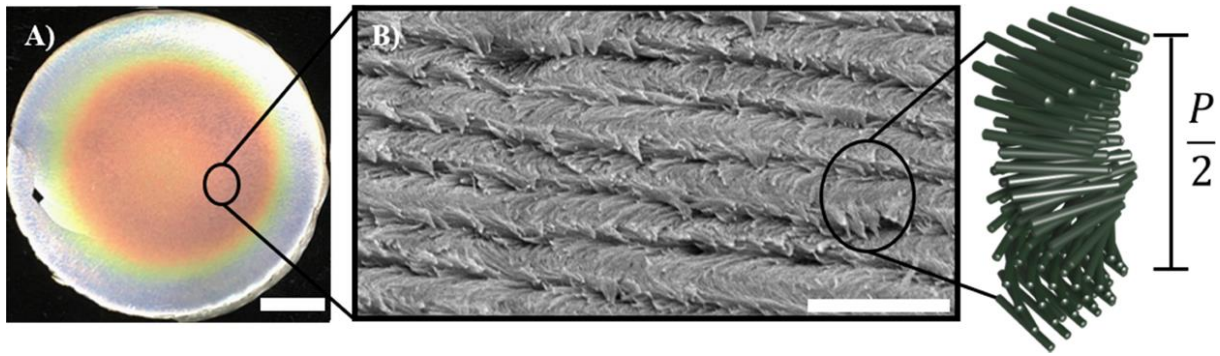
115

Above a particular concentration, CNC whiskers aggregate to form tactoids. While drying, they stack into layers. Each layer has a direction orthogonal to the nematic axis, and the layers are modulated to a helicoidal form (Dumanli et al., 2014) (Frka-Petesic et al., 2017), as shown in figure 3. The origin of the helicoidal arrangement is the chirality of CNC obtained due to D-glucose units (Tran et al., 2020). This specific structure displays CNC film with optical functionalities that favor its use in biophotonic material (Xiong et al., 2019).

120

Besides the optical properties, films based on nanocellulose show good mechanical properties compared to films made from other materials (tensile strength of 100–300 MPa and a modulus of 5–30 GPa) (Fang et al., 2019b). Thanks to their high surface area, they can be used as templates with other materials such as TiO<sub>2</sub>, carbon, and organosilica (Lagerwall et al., 2014). Therefore, integrating novel functionalities in the CNC structure can extend their application as films in many different fields.

124



125

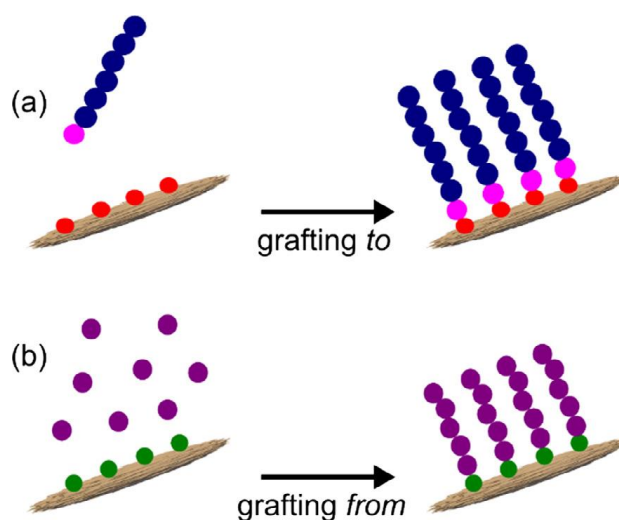
126 **Figure 3. (A) Photograph and (B) scanning electron microscopy (SEM) image of CNC film** (Tran et al.,  
 127 2018). John Wiley and Sons Copyright (2020).

128 **3. Chemical modification of cellulose nanocrystal**

129 Cellulose can be chemically modified via its hydroxyl groups, mainly the primary alcohol group. This modification  
 130 can broaden its application and improve its compatibility with other materials. Modification could be done  
 131 following different strategies depending on the species inserted.

132 **3.1. Graft polymerization**

133 Graft polymerization is considered a good approach to modifying the surface and endowing it with new physical  
 134 and chemical properties (Wohlhauser et al., 2018). It consists of attaching a sequence of monomers to the cellulose  
 135 backbone. The inserted polymer will give new properties to cellulose depending on its functional group (Roy et  
 136 al., 2009). Two main approaches are used for graft polymerization, the “grafting to” and the “grafting from”  
 137 approach (figure 4). The “grafting to” approach involves attaching a pre-formed polymer to the cellulose's  
 138 functional site via the polymer's reactive end group (Oberlintner et al., 2021). This approach can be limited because  
 139 of the steric hindrance; larger polymer chains can intertwine and prevent the functional group from reaching the  
 140 cellulose surface (Kedzior et al., 2019). While the “grafting from” consists of the immobilization of the initiator  
 141 on the cellulose surface to allow the polymer chain's growth. This approach is widely used because it provides a  
 142 high grafting density with a good control length (Wohlhauser et al., 2018) (Kedzior et al., 2019). The two  
 143 approaches can be applied by using different techniques such as atom transfer radical polymerization (ATRP),  
 144 reversible addition-fragmentation chain transfer (RAFT), nitroxide-mediated radical polymerization (NMP), ring-  
 145 opening polymerization (ROP), and free radical polymerization.

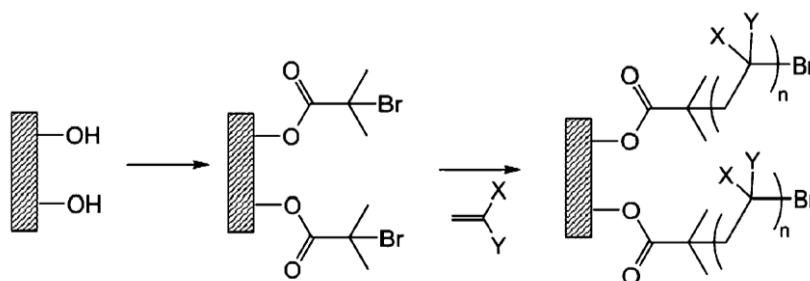


147  
148

149 **Figure 4. Schematic representation of (a) grafting to the CNC surface and (b) grafting from where**  
150 **polymerization is initiated from the CNC surface.** (Kedzior et al., 2019). Elsevier Copyright (2019).

### 151 3.1.1. Atom transfer radical polymerization (ATRP)

152 As its name implies, ATRP relies on the transfer of halogen atoms between a dormant species (R-X) and a  
153 transition metal catalyst  $M_i^n$ -X/ligand (Mishra & Kumar, 2012). The active radical is generated due to the transfer  
154 of the halogen atoms from the dormant species to a transition metal complex by oxidative addition. The radical  
155 created will then react with the monomer to further form a polymer chain (Roy et al., 2009).



156

157 **Figure 5. Modification of cellulose by grafting polymer via ATRP polymerization** (Roy et al., 2009) The  
158 **Royal Society of Chemistry, Copyright (2009).**

159 ATRP has been largely used to graft polymers to substrates due to its ability to form a well-controlled polymer  
160 chain with a high grafting density. A large panel of monomers was attached to cellulose nanocrystals, as  
161 summarized in table 1. The main way used to start the surface-initiated ATRP (SI-ATRP) is to first graft the  
162 initiator to the surface of CNC by esterification; the initiator usually applied are 2-Bromoisobutyryl bromide  
163 "BIBB" and  $\alpha$ -Bromoisobutyric acid "BIBA", then the polymer chain grows from the surface. The main negative  
164 point of using ATRP is the use of toxic transition metal complexes and the need to separate them from the final  
165 product. So, to overcome these drawbacks and decrease the amount of metal, Sèbe et al. used Activator Re-  
166 Generated by Electron Transfer ATRP (ARGET-ATRP) to graft polystyrene and poly(4-vinyl pyridine). This



167 approach uses a reducing agent in excess to regenerate the catalyst regularly from the deactivated form. By  
168 comparing ATRP and ARGET-ATRP, it has been observed that ARGET promotes the formation of a longer chain  
169 with a low grafting density; this is because the propagation step is fast, and the amount of the catalyst is of the  
170 order of ppm (Z. Zhang et al., 2019). Another approach was applied by Cunningham et al. to reduce the amount  
171 of catalyst, based on the use of Cu(0) as a reducing agent. The Cu(0) was added in the form of wire and was easily  
172 removed at the end. (Arredondo et al., 2017)

### 173 174 **3.1.2. Reversible addition-fragmentation chain-transfer (RAFT)**

175 RAFT is an effective process for controlling living radical polymerization; it enables the synthesis of  
176 macromolecular with complex architecture (Semsarilar & Perrier, 2010). It involves thiocarbonylthio compounds  
177 that serve as chain transfer agents. The effectiveness of this agent relies on the radical leaving group "R", the  
178 activating group "Z" and its compatibility with monomers (Moad et al., 2013). Table 2 regroups polymers with the  
179 corresponding RAFT agent used. The R group needs to be a good homolytic leaving group and be able to reinitiate  
180 new polymer chains. In contrast, the Z group must provide the RAFT agent with good resonance stabilization and  
181 polar effects to be more active (Tsang & Holdcroft, 2012). Grafting polymers to CNC by RAFT polymerization  
182 surface can be applied by immobilizing the RAFT agent to the surface via either the Z approach or the R approach.  
183 In the Z approach, the di(tri)thio group is permanently grafted to the cellulose surface while the chain grows aside.  
184 In the R approach, the polymer chain grows from the surface (Boujemaoui et al., 2016). Li et al. used another  
185 method to graft "PDMAEMA-*b*-PGMA-*b*-PHFBA "to the CNC surface. The polymer was first synthesized by  
186 RAFT, and then it was grafted onto cellulose via the reaction between the epoxy ring of PGMA and the hydroxyl  
187 group of the cellulose. The hydrophobicity increased, confirming successful grafting (J. Zhou et al., 2021).

### 188 **3.1.3. Ring-opening polymerization (ROP)**

189 ROP is a polymerization technique that involves monomers such as epoxides, cyclic esters (ex. lactones, lactides),  
190 and cyclic carbonates (Sarazin & Carpentier, 2015). ROP occurs following mechanisms such as radical, cationic,  
191 anionic, and ring-opening metathesis polymerization (Nuyken & Pask, 2013). It mainly depends on the monomer,  
192 catalytic system, and the initiator used (Carlmark et al., 2012). The hydroxyl group can be used as an initiator for  
193 ROP. Thus modification of cellulose using ROP seems interesting (Carlsson et al., 2015) since no prior chemical  
194 treatment will be needed (Carlmark et al., 2012). Grafting PLA from CNC surface was extensively studied using  
195 Tin (II) octoate as a catalyzer (Table 3); this grafting aims to enhance CNC's ability to adhesion with another  
196 polymer matrix to improve its properties.

197  
198

Modified CNC	Polymer	Grafting Method	Reference
CNC-g-PMMAZO	Poly{6-[4-(4-methoxyphenylazo) phenoxy] hexyl methacrylate} (PMMAZO)	Grafting from	(Q. Xu et al., 2008)
CNC-g-PDMAEMA	Poly (N, N-dimethylamino ethyl methacrylate) (PDMAEMA)	Grafting from	(Yi et al., 2009) (Morits et al., 2018) (Rosilo et al., 2014) (Hu et al., 2016) (Arredondo et al., 2017)
CNC-g-PS	Polystyrene (PS)	Grafting from	(Z. Zhang, Tam, et al., 2018)(Morandi et al., 2009)
CNC-g-PEGEEMA	Poly (poly (ethylene glycol) ethyl ether methacrylate) (PEGEEMA)	Grafting from	(Hu et al., 2016)
CNC-g- P(PEGMA)	Poly (poly (ethylene glycol) methylacrylate) (P(PEGMA)	Grafting from	(X. Zhang et al., 2017)
CNC-g- PDEAEMA	Poly (diethyl aminoethyl methacrylate) (DEAEMA)	Grafting from	(Arredondo et al., 2017)
CNC-g-PNIPAAm	Poly(N-isopropyl acrylamide) (PNIPAAm)	Grafting from	(Zoppe et al., 2017)
CNC-g-PMETAC	Poly [2-(methacryloyloxy)ethyl]- trimethylammonium chloride (PMETAC)	Grafting from	(Zoppe et al., 2017)
CNC-g-PSS	Poly (sodium 4-vinylbenzenesulfonate) (PSS)	Grafting from	(Zoppe et al., 2017)
CNC-g-P(AzoC6MA-co-DMAEMA)	AzoC6MA PDMAEMA	Grafting from	(Yuan et al., 2018)
CNC-g-PBA	Poly (butyl acrylate)	Grafting from	(Kedzior et al., 2018)
CNC-g-P4VP	Poly(4-vinyl pyridine) (P4VP)	Grafting from	(Liangjiu Bai et al., 2019)(Z. Zhang, Sèbe, et al., 2018a)
CNC-g-P(NIPAAm-co-HDPAP)	PNIPAM 6,6'- (hydrazine-1,2 diylidene bis (phenyl methanylylidene))- bis(3-(allyloxy) phenol) (PHDPAP)	Grafting from	(Junyu Chen et al., 2020)
CNC-g-PFAZO	Poly(9-[4-[2-[4-(trifluorometh) phenyl] diazenyl] phenoxy] nonayl acrylate) (PFAZO)	Grafting from	(Z. Xu et al., 2020)
CNC-g-PBA	Poly (butyl acrylate) (PBA)	Grafting from	(Kiriakou et al., 2021)
CNC-g-POEGMA	Poly (Hydroxyl oligo ethylene glycol methacrylate) (POEGMA)	Grafting from	(Dupont et al., 2021)(Grishkewich et al., 2016)
CNC-g-PCEM	Poly (cinnamoyl ethyl methacrylate) (PCEM)	Grafting from	(Z. Zhang, Sèbe, et al., 2018b)
CNC-g-PBMA	Poly(butyl methacrylate) (PBMA)	Grafting from	(Boujemaoui et al., 2017)

199

200

**Table 1. Summary of polymers grafted to CNC via ATRP.**

Modified CNC	Agent RAFT	Polymer	Grafting Method	Reference
CNC-g-PVPy	4-cyano-4-(isopropoxycarbonothioylthio)pentanoic chloride	Poly(N-vinylpyrrolidone) (PVPy)	Grafting from	(X. Qin et al., 2021)(Ge et al., 2021)
CNC-g-(PDMAEMA-b-PGMA-b-PHFBA))	S-1- Dodecyl-S'-( $\alpha$ , $\alpha'$ -dimethyl- $\alpha''$ -acetic acid) trithiocarbonate	Poly(2-(dimethylamino) ethyl methacrylate)-b-poly (glycidyl methacrylate)-b-poly (2,2,3,4,4,4-hexafluorobutyl acrylate) PDMAEMA-b-PGMA-b-PHFBA)	Grafting to	(J. Zhou et al., 2021) (J. Zhou et al., 2019) (Hong Li et al., 2020)
CNC-g-PDMAEMA	4-cyano-4-((phenylcarbonothioyl)-thio)pentanoic acid	Poly (dimethylaminoethyl methacrylate) (PDMAEMA)	Grafting from/ Grafting to	(Arredondo et al., 2020)
CNC-g-PDEAEMA	4-cyano-4-((phenylcarbonothioyl)-thio)pentanoic acid	Poly (diethyl aminoethyl methacrylate) (PDEAEMA)	Grafting from/ Grafting to	(Arredondo et al., 2020)
CNC-g-PDPAEMA	4-cyano-4-((phenylcarbonothioyl)-thio)pentanoic acid	Poly (diisopropylaminoethyl methacrylate) (PDPAEMA)	Grafting from/ Grafting to	(Arredondo et al., 2020)
CNC-g-(PDMAEMA-b-NIPAAm)	S-(thiobenzoyl)thioglycolic acid	Poly (N-isopropylacrylamide) (PNIPAAm) Poly (2-dimethylaminoethyl) methacrylate (PDMAEMA)	Grafting from/Grafting to	(Eskandari et al., 2020)
CNC-g-(BA-co-VI)	Macro CTA	Poly(n-butyl acrylate-co-1-vinyl imidazole)	Grafting from	(Wentao Wang et al., 2020)
CNC-g-P(DMAEMA-co-C)	S-(thiobenzoylthioglycolic) acid	Poly (2-dimethylaminoethyl) methacrylate (PDMAEMA) Pcoumarin	Grafting from	(Abousalman-Rezvani et al., 2019)
CNC-g-(PAA-b-PHFBA)	S-Benzyl-S'-trimethoxysilylpropyltrithiocarbonate	Polyhexafluorobutyl acrylate (PHFBA) Polyacrylic Acid (PAA)	Grafting to	(Yao et al., 2019)
CNC-g-PVAc	2-((Ethoxycarbonothioyl)thio)propanoic acid	Poly (vinyl acetate) (PVA)	Grafting from	(Boujemaoui et al., 2016)
CNC-g-PMMA	4-cyano-4-(phenylcarbonothioylthio)pentanoic acid	Poly (methyl methacrylate) (PMMA)	Grafting from	(Anžlovar et al., 2016)
CNC-g-P(NIPAAm-co-AA)	2-(dodecylthiocarbonothioylthio)-2-methyl propionic acid	Poly (acrylic acid) (PAA) Poly(N-isopropyl acrylamide) (PNIPAAm)	Grafting from	(Zeinali et al., 2014) (Zeinali et al., 2018)
CNC-g-(PNIPAAm-b-PAA)	S-(thiobenzoylthioglycolic) acid	Poly (acrylic acid) (PAA) Poly(N-isopropyl acrylamide) (PNIPAAm)	Grafting from	(Haqani et al., 2017)
CNC-g-PAM	Macro CTA	Polyacrylamide	Grafting from	(T. Liu et al., 2017)(T. Liu et al., 2016)
CNC-g-PDMA	Macro CTA	Poly(N,N-dimethyl acrylamide)	Grafting from	(T. Liu et al., 2017) (T. Liu et al., 2018)

**Table 2. Summary of polymers grafted to CNC via RAFT.**

203

Modified CNC	Polymer	Grafting Method	Reference
CNC-g-PO <sub>x</sub>	<i>Poly(2-oxazoline)</i>	Grafting to	(Gauche & Felisberti, 2019)
CNC-g-PEEP	<i>Poly(ethyl ethylene phosphate)</i>	Grafting to	(H. Wang et al., 2015)
CNC-g-PLA	<i>Poly(Lactide)</i>	Grafting from	(Jianxiang Chen et al., 2017) (Goffin et al., 2011)(Miao & Hamad, 2016)(Lizundia et al., 2016)(Habibi et al., 2013) (H. Wu et al., 2016)
CNC-g-P(CL-co-LA)	<i>Poly(D-lactide-co-<math>\epsilon</math>,caprolactone)</i>	Grafting from	(Muiruri et al., 2017)
CNC-g-PLA6	<i>Poly(caprolactam) (Polyamide 6)</i>	Grafting form	(Rahimi & Otaibge, 2016)(Kashani Rahimi & Otaigbe, 2016)
CNC-g-PCL	<i>Poly(<math>\epsilon</math>-caprolactone)</i>	Grafting from	(Carlsson et al., 2015)

204  
205

**Table 3. Summary of polymers grafted to CNC via ROP.**

#### 206 **3.1.4. Nitroxide-mediated polymerization (NMP)**

207  
208 NMP is based on the use of nitroxide to initiate the polymerization without the implication of another radical  
209 source or the need for a metal catalyst. The main characteristic of the alkoxyamine that could be used for NMP is  
210 its ability to provide reactive radical to initiate polymerization and form a stable mediating nitroxide radical. NMP  
211 can be used to graft polymer on a natural surface such as cellulose. For the "grafting from" approach, CNC can be  
212 functionalized with nitroxide forming, thus an alkoxyamine able to induce polymerization. Roeder and co-workers  
213 first graft BlocBuilder® (BB) on CNC via a covalent bond to the vinyl group of 4-chloromethyl styrene (CMS)  
214 that was already inserted into CNC. The polymerization was generated after adding the monomer (Roeder et al.,  
215 2016). The "Grafting to" approach was applied by Glasing et al., where they first modified CNC with glycidyl  
216 methacrylate (GMA). The polymerization was generated in the presence of macroalkoxyamines based on N-  
217 hydroxysuccinimidyl BlocBuilder® and polymers such as Styrene, N, N-(diethylamino)ethyl  
218 methacrylate (DEAEMA), and N-3-(dimethylamino)ethyl methacrylamide (DMAPMAm) (Glasing et al., 2017).

#### 219 **3.1.5. Free-radical polymerization (FRP)**

220 FRP is an uncontrolled polymerization technique, and the synthesized polymers usually have a high dispersity.  
221 Several methods initiate FRP, such as chemical, thermal, and radiation. Jeun and co-workers successfully grafted  
222 1H,1H,2H,2H-perfluorodecyl acrylate (PFDA) using electron beam (e-beam) irradiation as a technique to initiate  
223 the polymerization. The advantage of e-beam is that it avoids the application of harmful compounds (Jeun et al.,  
224 2019). Plasma was also applied to graft polymers on CNC surfaces. Here, we can cite the research done by  
225 Alanis et al. where they graft different monomers (caprolactone, styrene,  $\alpha$ -farnesene) (Alanis et al., 2019). The  
226 main advantage of this technique is the possibility of polymerizing a wide range of monomers.

### 227 **3.2. Grafting small molecule**

228  
229 Grafting small molecules on the CNC surface is advantageous. Diverse functions can be grafted using reactions  
230 with suitable conditions and high yield. Many strategies are applied; we discussed below click chemistry, silylation  
231 and esterification.

#### 232 **3.2.1. Click chemistry**

233  
234 Click chemistry was first introduced by Sharpless et al. in 2001, describing reactions that satisfy the following  
235 criteria: stereospecific, giving high yields, modular, wide in scope, implies simple experimental conditions, the  
236 product should be easily isolated and involve only benign solvent if it is necessary (Kolb et al., 2001). The  
237 commonly used click chemistry reactions are Diels-Alder, thiol-ene, the azide-alkyne Huisgen, and the Cu<sup>1</sup>-  
238 catalyzed azide-alkyne cycloadditions (Filpponen, 2014). Click chemistry was used to modify CNC by either

239 bringing two CNC chains together (Filpponen, 2014) or grafting new functionalities to its surface. CNC can be  
 240 functionalized with an Azide or an alkyne functional group for the Azide-alkyne cycloaddition, and Thiol-ene  
 241 click chemistry CNC should be modified with thiol function or a methacrylate (Table 4).

Modified CNC	Inserted species	Click-reaction	Ref
CNC-Azide	CNC-alkyne	Cu(I)-catalyzed Huisgen 1,3-dipolar	(Filpponen, 2014)
CNC-Azide	Propargyl-terminated poly(ethyl ethylene phosphate) (propargyl-PEEP)	Cu(I)-catalyzed azide-alkyne cycloaddition (CuAAC)	(H. Wang et al., 2015)
CNC-Azide	Polycaprolactone diol-C≡CH	(CuAAC)	(L. Zhou et al., 2018)
Fe <sub>3</sub> O <sub>4</sub> /CNC-Azide	Propargyl alcohol	(CuAAC)	(Movagharnegad et al., 2018)
CNC-methacrylate	1H,1H,2H,2H-perfluorodecanethiol	Thiol-ene	(Aalbers et al., 2019)
CNC-SH	N-phenyl maleimide	Thiol-ene	(J. L. Huang et al., 2014)
CNC-alkyne	Azide-polycaprolactone diol	(CuAAC)	(L. Zhou et al., 2019)

242 **Table 4. Summary of species grafted to CNC via Click reactions**

### 243 3.2.2. Silylation

244  
 245 CNC can be modified by inserting a Siloxane group to enhance the hydrophobicity of cellulose (Anpilova et al.,  
 246 2020) and increase the thermal stability of the modified CNC (Khanjanzadeh et al., 2018). Zanata et al. developed  
 247 crosslinked aerogels based on cellulose nanocrystals using 3-isocyanatopropyltriethoxysilane (IPTS), the  
 248 developed material exhibit an amphiphilic character (De Morais Zanata et al., 2018). Silylation of CNC can have  
 249 another purpose: endowing nanocellulose with flame retardancy. In this sense, Kim and co-workers modified CNC  
 250 with Tris(2-chloroethyl) phosphate (TCEP) to incorporate it into a polyurethane matrix, and the result showed an  
 251 increase in the limiting oxygen index up to 28% (Kim et al., 2020). To enhance CNC adsorption capacity toward  
 252 CO<sub>2</sub>, Zhu et al. modified it with 3-(2-aminoethylamino)-propyl methyl dimethoxy silane (APS); the results  
 253 revealed that even after ten cycles of adsorption and desorption the adsorption capacity remained above 85% which  
 254 emphasize the APS-CNC aerogel potential to adsorb CO<sub>2</sub> (W. Zhu et al., 2020). Incorporating organosilane-  
 255 modified cellulose nanocrystal into natural rubber matrix proves its efficiency in improving mechanical properties  
 256 of the latter; as Singh and co-workers showed in their research (Singh et al., 2020).

### 257 3.2.3. Esterification

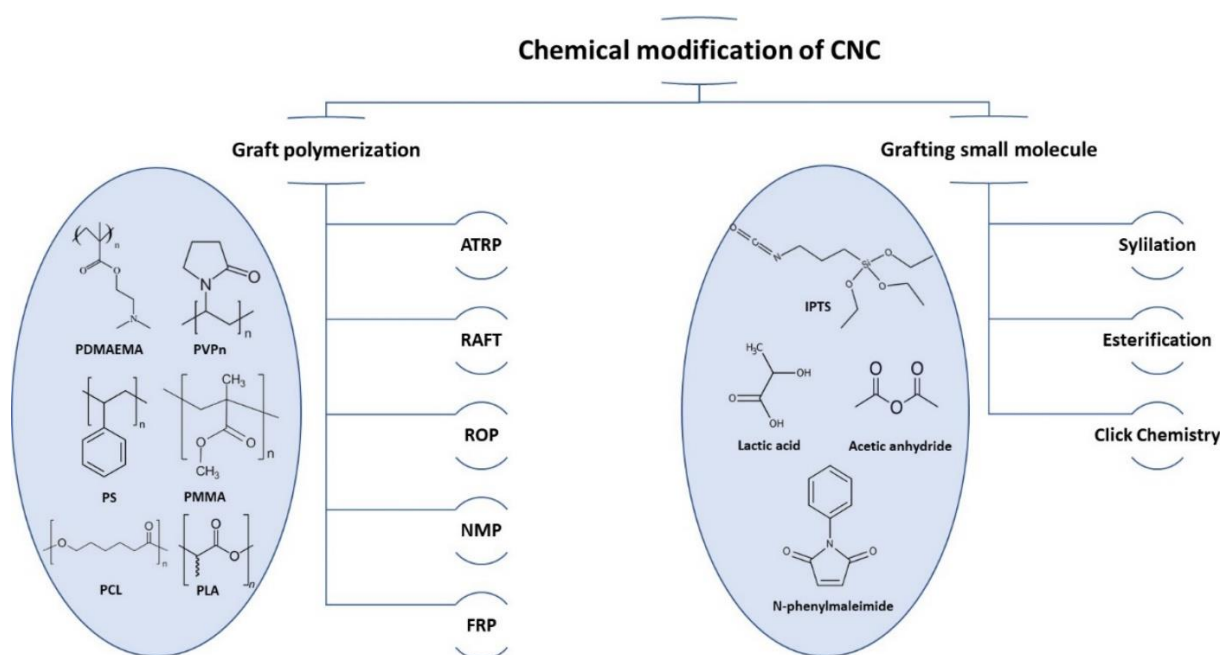
258  
 259 The modification of cellulose nanocrystals by esterification is an interesting method to modify CNC, as  
 260 summarized in table 5. Esterification can be applied using a variety of catalysts such as sulphuric acid, hydrochloric  
 261 acid, iodine, potassium carbonate, and triethylamine, to name a few (Ávila Ramírez et al., 2017). The degree of

262 substitution (DS), defined as the average number of substituent groups graft per base unit (anhydroglucose unit)  
 263 for cellulose the DS may range from zero to three since it has three reactive hydroxyls (Wiley & Sons, 2011),  
 264 depending on the concentration of the reagents, the concentration of catalyst and the removal of water (Abraham  
 265 et al., 2016).

266

Grafted species	Degree of substitution	Usage	References
Canola oil fatty acid methyl ester	0.5	Hydrophobic coating agent	(Wei et al., 2017)
Acetic anhydride	2.18	Reinforcing nanocomposite	(Abraham et al., 2016)
Lauroyl chloride	0.2-2.4	Reinforcing nanocomposite	(Trinh & Mekonnen, 2018)
Succinic anhydride	1.6-2.2	Dye removal	(Emam & Shaheen, 2019)
Acetic anhydride	0.18-0.34	Reinforcing nanocomposite	(Ávila Ramírez et al., 2017)
Vinyl acetate- Vinyl cinnamate	-	Emulsifying agents	(Seibe et al., 2013)
Palmitoyl chloride	0.3-0.8	Improve dispersibility	(Fumagalli et al., 2013)
Long-chain aliphatic acid chlorides	-	Reinforcing nanocomposite	(Bendahou et al., 2015)
Phenylacetic acid	0.5	Composite manufacturing	(Espino-Pérez et al., 2014)
Benzylacetic acid	0.3		
Rosin	-	Anti-microbial activity	(De Castro et al., 2016)
Malonate	0.16	Reinforcing nanocomposite	(Spinella et al., 2016)
Malate	0.22		
Citrate	0.18		
Lactic acid	87.7%	Reinforcing nanocomposite	(H. Wu et al., 2018)
Malic acid	0.035-0.20	Reinforcing nanocomposite	(Wei Wang et al., 2018)
Valeric acid	0.35	Reinforcing nanocomposite	(Shojaeiarani et al., 2019)
Succinic anhydride	0.12-0.32	Reinforcing nanocomposite	(Leszczyńska et al., 2019)
Octenyl Succinic Anhydride	0.539-0.768	Adsorption of Cu(II) ions	(Gupta et al., 2019)
3-thiophenetic acid	1.1	Increase planarity of the conjugated polymer chains	(Silva et al., 2021)

**Table 5. Summary of species grafted to CNC via esterification, with the degree of substitution obtained and their different usage.**



267

268 **Figure 6: Schematic representation resuming strategies of chemical modification of CNC with some**  
 269 **grafted species**

270 **4. Nanocomposite film and membrane-based on cellulose nanocrystal**

271 **4.1. Preparation of cellulose nanocrystal composite film and membrane**

272 Cellulose nanocrystals can be used as templates with the ability to form mesoporous films (Y. Huang et al., 2020).  
 273 The significant problems CNC films face are their brittleness and poor water resistance that prevent their  
 274 applications. Huang et al. developed a flexible composite film using poly (ethylene glycol) diacrylate (PEGDA)  
 275 to overcome this issue. PEGDA encapsulates CNC by forming a three-dimensional crosslinking network.  
 276 PEGDA was mixed with a photoinitiator, then added to a CNC suspension and cast in a plastic Petri dish. The film  
 277 was obtained by evaporation-induced self-assembly (EISA); by the end of this step, CNC and PEGDA interacts  
 278 via hydrogen bonding. To stimulate the encapsulation of PEGDA to CNC, the film was exposed to UV. It was  
 279 observed that the tensile strength decreased with the increasing amount of PEGDA, while the flexibility of the  
 280 composite film has been improved compared to the pristine CNC film. After soaking the prepared film for 24 h,  
 281 its structure was preserved, which shows its good water-resistant property. The three-dimensional structure of the  
 282 developed film allows its applications as a water-content detector, anti-counterfeiting label, and photonic paper  
 283 (Y. Huang et al., 2020).

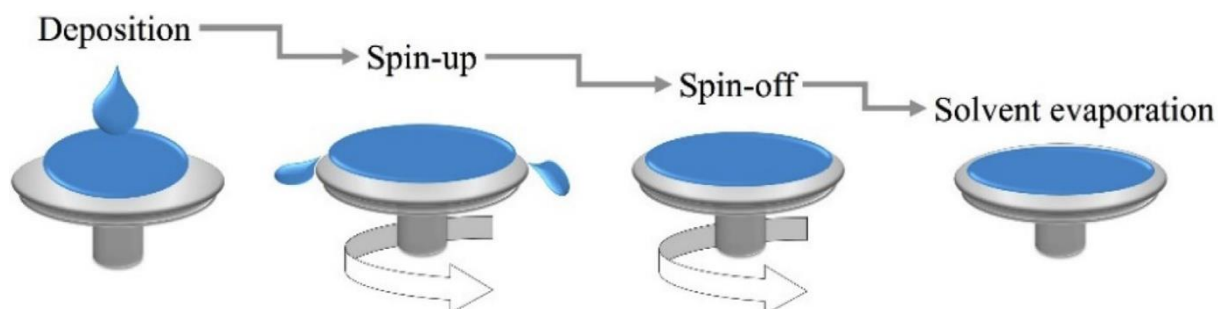
284 To avoid the coffee-ring phenomenon obtained due to the heterogeneity structure while the drying process, Zhang  
 285 et al. used vacuum-assisted self-assembly (VASA) to help obtain a well-oriented and structurally homogeneous  
 286 CNC film. CNC suspension was filtered using poly(tetrafluoroethylene) (PTFE) as a support membrane under



287 vacuum. After filtration and completely drying, CNC film was peeled off from PTFE. The effect of prior sonication  
288 and the volume of suspension was evaluated to emphasize their impact on the iridescent of the obtained film. It  
289 was reported that the sonication duration does not impact CNC crystallinity, but it is responsible for the coloration  
290 variation of the films obtained. A long sonication time is needed to obtain an iridescent CNC film via VASA. Beck  
291 et al. reported that sonication leads to the rejection of ions from the bound-water layer, which leads to a large pitch  
292 because of the weak chiral interaction between CNC particles (Beck et al., 2011). The amount of CNC also  
293 impacted the chiral nematic structure of the film. While changing the suspension volume, films with different  
294 colors were obtained, suggesting that the chiral nematic structure's helical pitch varies with the CNC film's  
295 thickness. The formation kinetics of CNC film also impact the iridescent of the latter so that varying the vacuum  
296 degree induces a color change (Q. Chen et al., 2014).

297 Vacuum filtration was used by Sulaiman et al. to prepare a nanocomposite film using a **layer-by-layer** approach.  
298 The group developed a bi-layer electrode using as layers polypyrrole/ graphene oxide (GO) and polypyrrole/CNC.  
299 The bilayer was prepared by first depositing PPy/ GO layer on a membrane filter via vacuum filtering and then  
300 adding the second layer PPy/CNC by applying vacuum filtration. After each deposition, the layers were washed  
301 with deionized water (Kulandaivalu & Sulaiman, 2020). Wagberg et al. reported that skipping the rinsing step will  
302 gender a rougher and less-defined layer (Wågberg & Erlandsson, 2021). After drying, the free-standing film was  
303 peeled off from the membrane. Multilayer film can be assembled via electrostatic interaction, hydrogen bonding,  
304 hydrophobic, and covalent bonding (Kulandaivalu & Yusran, 2019). Herein the interaction between the two layers  
305 was insured by hydrogen bonding between the oxygen in GO and the hydroxyl group of CNC. The assembly of  
306 the two layers PPy/GO|PPy/CNC induced active sites, which attributed to the generated film's high surface area  
307 (Kulandaivalu & Sulaiman, 2020). In the same context, Xia et al. developed a tri-layer membrane using mid-layer  
308 polydimethylsiloxane (PDMS), surrounded by two layers of nanocrystals cellulose modified with  
309 methyltrimethoxysilane. The silylation was intended to render the CNC surface hydrophobic and increase its  
310 dispersion in PDMS. The modification did not impact the crystallinity of CNC, which endowed the PDMS matrix  
311 with rigidity, one of the fundamental properties of CNC that favored its use as a reinforcing agent. The three layers  
312 were covalently bonded due to the crosslinking curing reaction applied during the preparation of the layers that  
313 provide strong adhesion between the layers. Barrier performance of the multilayer membrane improved compared  
314 with neat PDMS material; it was noted that oxygen permeability decreased due to the presence of Si-CNC, which  
315 was explained by the fact that Si-CNC nanoparticles block O<sub>2</sub> from diffusing while crossing the composite layers  
316 (Xia et al., 2018).

317 Shojaeiarani et al. developed a nanocomposite film based on poly (lactic acid) and CNC using EISA and **spin**  
318 **coating**. A mixture of PLA-CNC was prepared in chloroform, injected into a spin coater plate, and kept for 180s  
319 under a constant spin speed of 150 rpm; the film was obtained after the evaporation of solvent at room temperature  
320 (figure 7). It was concluded that spin coating allows good dispersion of CNC due to the high drying rate, compared  
321 to EISA, which improves the degree of crystallinity and decreases the hydrophilicity (Shojaeiarani et al., 2020).



322  
323 **Figure 7. Formation of the film via the spin-coating method** (Shojaeiarani et al., 2020). Elsevier Copyright  
324 (2019).

325 **Electrospun** nanocomposite mats-based chitosan/Polyethyleneoxide /CNC was prepared by Nasri et al. using  
326 CNC isolated by hydrochloric acid or sulphuric acid to investigate the effect of surface functionalities of CNC.  
327 During the electrospinning process, it was observed that the jet was stable for the solution prepared with CNC  
328 (HCl), which led to the formation of fibers of good quality. In contrast, the fiber obtained by using CNC (H<sub>2</sub>SO<sub>4</sub>)  
329 was non-uniform. The mechanical properties increased with the reinforcement of the matrix fiber with both types  
330 of cellulose nanocrystals (Naseri et al., 2015). In another study by Nair et al., they reported a decrease in both  
331 tensile strength and Young's modulus for nanocomposite fiber mats based on CNC and Cellulose acetate (CA),  
332 and it was explained by the fact that CNC acted more defects due to the aggregation during the loading (Naseri et  
333 al., 2015).

#### 334 **4.2. Application of cellulose nanocrystal composite membrane and film**

335 Film and membrane have promising use in electronics, sensors, solar cells, water treatment, and so on. Several  
336 studies have been carried out in this direction. They have shown the possibility of integrating cellulose into  
337 different matrices to develop films with good performance depending on their field of application.

##### 338 **4.2.1. Conductive materials**

339 To endow cellulose with electrical properties, a conductive material such as conductive polymers (Polyaniline,  
340 Polypyrrole, etc.), metallic particles, and conductive carbon material was combined with cellulose, so the  
341 developed nanocomposite material exhibits properties of both materials (Du et al., 2017). Polyaniline (PANI), one  
342 of the conductive polymers, has drawn much attention due to its high electrical conductivity. However, PANI  
343 tends to aggregate, limiting its application (S. Wang et al., 2016)(Nepomuceno et al., 2021). PANI was synthesized

344 in the presence of other materials such as CNC to overcome this issue. Nepomuceno et al. synthesized PANI via  
345 in situ polymerization in the presence of CNC; the latter played the role of a backbone to PANI deposition. The  
346 group reported that while adding aniline to CNC, the amino group of aniline interacted with the hydrogen bond  
347 between the hydroxide group of CNC, which promoted the in-situ polymerization. The negative charge on the  
348 CNC surface interacted with positively charged amine groups of polyanilines which slowed the polymerization  
349 time. In other words, increasing the amount of aniline monomer enhanced the probability of polymerization  
350 occurring, thus decreasing the polymerization time. Increasing PANI concentration led to CNC coating, facilitating  
351 electrons' mobility. For a PANI/CNC ratio of 0.4, the conductivity obtained was  $8.9 \times 10^{-1} \text{ S cm}^{-1}$ ; this value matches  
352 the requirement for using sensors and electromagnetic interference shielding (Nepomuceno et al., 2021). To  
353 increase the stability of CNC/PANI, Wang et al. used cellulose nanofibers as a dispersant. The obtained film  
354 exhibits a conductivity of  $104.7 \text{ S cm}^{-1}$ . The group reported that the presence of CNF avoids the agglomeration of  
355 CNC and PANI (S. Wang et al., 2016). Wu et al. have also used polypyrrole with CNC to develop a nanocomposite  
356 material for supercapacitor application. To obtain a well-controlled and uniform coating of PPy, poly(N-vinyl-  
357 pyrrolidone) PVP was first adsorbed on the CNC surface to modify the hydrophilicity of CNC and favored the  
358 coating of PPy. PPy also acts as a stabilizer that inhibits the formation of aggregates. Due to hydrogen bonds  
359 between the carbonyl groups of PVP and the N-H group of pyrroles, the PPY growth uniformly on PVP-coated  
360 CNC. The core-shell PPy/PVP/CNC material exhibit a conductivity of  $36.9 \text{ S cm}^{-1}$  (X. Wu et al., 2014).  
361 Incorporating nanoparticles into CNC matrices enhances conductivity, as reported by El-Nahrawy et al. The group  
362 developed a nanocomposite material consisting of CNC coated with PPy and Ag Nanoparticles and ( $\text{Ni}_2\text{O}_3$ )  
363 nanoparticles. The formed material had unique electroconductive properties due to the support of PPy with the  
364 presence of an excess of charge carries (El-nahrawy et al., 2020).

#### 365 **4.2.2. Water treatment**

366 Nanocomposite membranes are promising materials for mitigating fouling and compromise between selectivity  
367 and permeability. Cellulose nanocrystal presents an excellent material to be part of this nanocomposite membrane,  
368 so the last can exhibit all the properties mentioned. The choice of cellulose nanocrystal is because they can be  
369 easily functionalized with other moieties to enhance their efficiency in retaining pollutants. Moreover, their  
370 hydrophilic nature due to the presence of hydrophilic groups can help mitigate fouling (C. Xu et al., 2020). The  
371 presence of CNC contributes to the membrane's good mechanical properties by increasing the tensile strength  
372 (Cruz-Tato et al., 2017), and it is favored over other nanoparticles because it is considered a renewable, non-toxic,

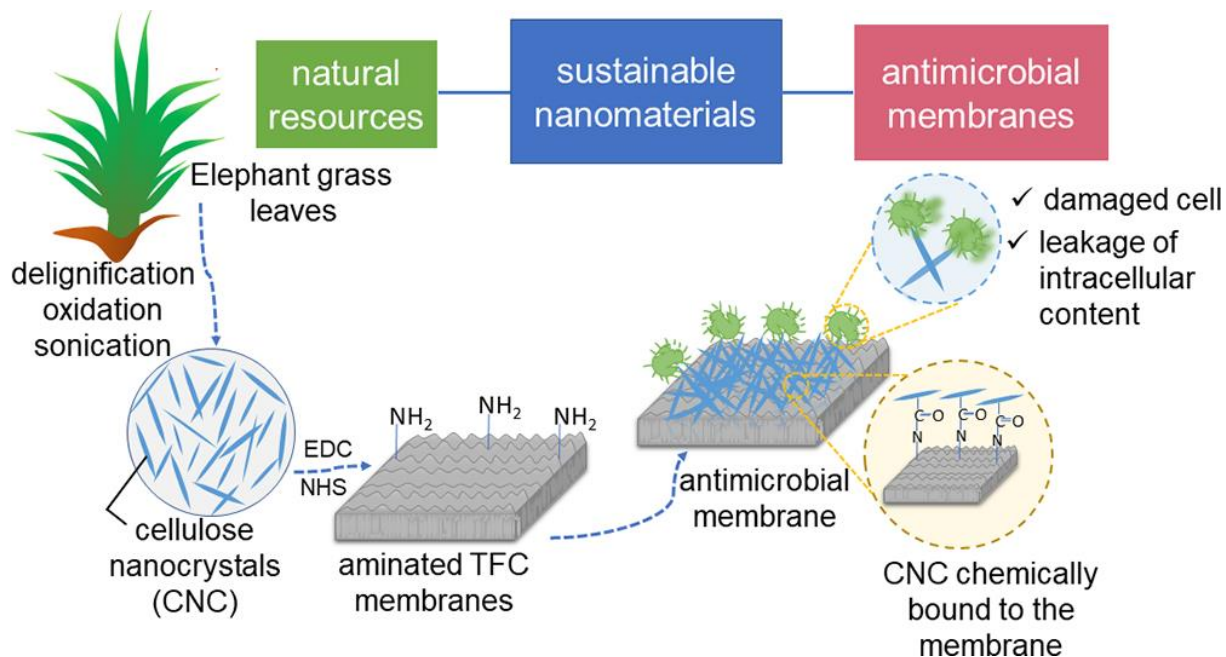
373 and biodegradable material (Asempour et al., 2018) solving thereby leaching problem related to toxic  
 374 nanoparticles.

Composite material	%CNC	Pollutants	Removal rate	Reference
PES	2 % (wt%)	<i>Humic acids (HAs)</i> <i>Bovine serum albumin (BSA)</i>	71.9% (HA) 82.7% (BSA)	(Langming Bai et al., 2020)
PES	5.5 $\mu\text{g}/\text{cm}^2$	<i>Heavy metal ions</i>	98 % ( $\text{CuSO}_4$ ) 96.5% ( $\text{CuCl}_2$ ) 90.8% ( $\text{PbCl}_2$ )	(Hoang et al., 2020)
PA/PES	0.01 wt% CNC/Ag	<i>Salt</i> <i>Bacteria</i>	99.1% ( $\text{Na}_2\text{SO}_4$ ) 99.4% ( <i>Escherichia Coli</i> )	(C. Xu et al., 2020)
PA	-	<i>Bacteria</i>	~ 89% ( <i>Escherichia Coli</i> )	(Jackson et al., 2021)
PA	0.1% (w/v)	<i>Salt</i>	97.8%	(Asempour et al., 2018)
PES	1 wt%	<i>Color</i> <i>Chemical oxygen demand (COD)</i>	94 % (color) 88 % (COD)	(Janoobi et al., 2019)
PA/PLS	0.05 wt%	<i>Salt</i>	98.3% ( $\text{Na}_2\text{SO}_4$ ) 96.1% ( $\text{MgSO}_4$ )	(S. Huang et al., 2019)
PVDF	4 wt%	<i>Oil/water</i>	97% of separation	(X. Wang et al., 2019)
Cellulose ester	26.7 $\text{mg}\cdot\text{ml}^{-1}$	<i>Antibiotic</i>	89% <i>Tetracycline hydrochloride</i>	(J. Liu et al., 2020)
Chitosan	90 wt%	<i>Dyes</i>	98% ( <i>Victoria Blue 2B</i> ) 84% ( <i>Methyl Violet 2B</i> ) 70% ( <i>Rhodamine</i> )	(Karim et al., 2014)
Cellulose Sludge/ CNF	-	<i>Heavy metal ions</i>	0.87 $\text{mg g}^{-1}$ ( $\text{Ag}^+$ ) 374 $\text{mg g}^{-1}$ ( $\text{Cu}^{2+}$ ) 456 $\text{mg g}^{-1}$ ( $\text{Fe}^{2+}/\text{Fe}^{3+}$ )	(Karim et al., 2017)
Cu mesh	-	<i>Aqueous crude oil mixture</i>	-	(M. B. Wu et al., 2019)
PES	-	<i>Aqueous crude oil emulsion</i>	-	(M. B. Wu et al., 2019)
PA	-	$\text{Na}_2\text{SO}_4$	96.7%	(J. J. Wang et al., 2017)
GO/PA	-	$\text{Na}_2\text{SO}_4$	94.2%–97.2%	(C. Y. Zhu et al., 2021)

375 **Table 6. Summary of composite membranes based on CNC for water treatment with the targeted**  
 376 **pollutants and the removal rate**

377 CNC was incorporated with different materials such as polyethersulfone (PES), polyamide as an active layer (PA),  
 378 polysulfone (PSF), and polyvinylidene fluoride (PVDF), among others to remove diverse pollutants (Table 6).  
 379 Several researchers used PES to develop nanocomposite membranes due to its high thermal stability and chemical  
 380 resistance in organic solvents (Langming Bai et al., 2020). Janoobi et al. developed a nanocomposite membrane  
 381 based on PES and CNC to remove color and reduce chemical oxygen demand from industrial wastewater. The

382 group first modified CNC with (3-aminopropyl) triethoxysilane (APTES), then mixed it with polyethersulfone  
383 polymer. The membrane was then prepared based on this blend solution. Adsorption tests showed that the presence  
384 of CNC enhanced the removal of color and contributed to the reduction of chemical oxygen demand. The  
385 adsorption was ensured by hydrogen interaction between hydroxyl groups of CNC and the different groups of the  
386 colored compounds. The presence of amino group from APTES help increase the removal of color due to its  
387 interaction with anionic groups of color, so they play the role of new adsorption sites (Jonoobi et al., 2019). Another  
388 reason to prepare composite membranes using CNC is to prevent fouling. Bai et al. used CNC due to its hydrophilic  
389 property. Comparing composite membrane based on CNC and PES to neat PES membrane, they note that the  
390 composite membrane is more hydrophilic, has a higher porosity than the neat one, and exhibits good performance  
391 in terms of antifouling ability. However, the excess of CNC renders the membrane surface rough due to the poor  
392 dispersibility of high concentrated solution of CNC, which impact the porosity and the permeability of the  
393 nanocomposite membrane too (Langming Bai et al., 2020). To endow a nanofiltration membrane with antifouling  
394 and antibacterial properties, Xu et al. prepared a composite membrane by incorporating CNC and Ag nanoparticles  
395 into an active polyamide layer, and PES was applied as the support material for this active layer. The developed  
396 membrane exhibits good antifouling and antibacterial performance and helps reduce energy consumption known  
397 for the nanofiltration process due to the enhancement in water flux and salt rejection (C. Xu et al., 2020). In the  
398 study by Jackson et al., CNC was used only as an anti-microbial agent and incorporated into the membrane; the  
399 result showed the inactivation of up to 89% of *Escherichia Coli*. The group relates the anti-microbial activity of  
400 CNC to its rod-like morphology that damage the cell membrane of the bacteria after contact (figure 8) (Jackson et  
401 al., 2021).



402

403 **Figure 8. Representative scheme of membrane-based on CNC with antibacterial activity** (Jackson et al.,  
 404 2021). American Chemical Society Copyright (2021).

405 **4.2.3. Packaging**

406 CNC has been widely used in packaging as a reinforcing material. Due to the CNC network, the mechanical  
 407 properties of the reinforced material improve significantly (S. Liu et al., 2019). Furthermore, this network plays  
 408 the role of a barrier to water vapor and oxygen, one of the crucial criteria for selecting the packaging material.  
 409 Packaging films based on CNC blending with PLA and PVA were extensively studied and showed promising  
 410 results in thermal stability, stiffness, and anti-microbial activity. (Pal et al., 2019) reinforced PLA with CNC and  
 411 reduced graphene oxide (rGO). The developed film exhibited a higher crystallinity due to the strong physical  
 412 interaction between CNC and PLA. Thus, the crystallinity increase reduces the water vapor permeability value.  
 413 (Salmieri et al., 2014) developed a bioactive packaging film based on CNC-PLA coated by nisin, the results  
 414 showed a promising inhibiting capacity against *Listeria monocytogenes*. On the other hand, (Dey et al., 2021)  
 415 emphasize the antifungal property of CNC, incorporated into PVA film, against postharvest pathogens. The study  
 416 showed the potential application of CNC for the packaging of fresh fruits. CNC was incorporated into other natural  
 417 polysaccharides, such as alginate, chitosan, and carrageenan (Yadav et al., 2019). In general, polysaccharides are  
 418 a promising material for packaging due to the considerable advantages they present as the preservation of aromas,  
 419 inhibition of oxygen penetration, and water absorption, not to mention their abundance and price (Hui Li et al.,  
 420 2020).

421 **4.2.4. Biomedical**

422 CNC has been known to be biocompatible and non-toxic for biomedical applications. It can be used for artificial  
423 blood vessels, tissue engineering (Dugan et al., 2010), drug delivery(Lin et al., 2016), etc. (Zeimaran et al., 2019)  
424 reinforced urethane with CNC to develop a self-healing nanocomposite film. The developed material showed an  
425 excellent cytocompatibility toward human dermal fibroblasts, making it promising for application in material  
426 engineering. In a more concrete study, (L. Qin et al., 2020) introduced CNC into a collagen-based film for corneal  
427 repair. The film was tested in vitro on rabbit corneal epithelial cells and keratocytes. The film showed its  
428 effectiveness in promoting epithelial wound healing and inhibiting keratocyte-myofibroblast transformation,  
429 which emphasizes CNC's potential to be applied as reinforcing agent material for corneal regeneration and  
430 reconstruction. A film based only on CNC can also be applied for medical purposes. As the study by (Prathapan  
431 et al., 2018) affirmed, the researchers prove the ability to use CNC film for blood typing. Despite all these  
432 advantages, the nanotoxicity of CNC needs to be more investigated since some studies reported some possible  
433 CNC toxic outcomes (Seabra et al., 2018).

#### 434 **5. Summary**

435 Cellulose is the most abundant biopolymer that can replace petroleum-based materials that harm health and the  
436 environment. CNC can be extracted from native cellulose and is known for its important mechanical properties  
437 (similar to Kevlar), surface reactivity, and its ability to self-assemble. Chemical modification of CNC broadens its  
438 application in different domains of material science and enhances its compatibility with other materials.  
439 Developing film and membrane based on CNC or modified CNC is a good solution to minimize the use of non-  
440 biodegradable material. These films and membranes could be used in various applications such as biosensors,  
441 electrodes, and membranes for water treatment, to name a few. Developing composite material from CNC could  
442 provide solutions to a broad range of technological bottlenecks in the industry and replace toxic materials currently  
443 being banned from use due to their impact on human health and environmental issues.

#### 444 **Reference**

445 Aalbers, G. J. W., Boott, C. E., D'Acerno, F., Lewis, L., Ho, J., Michal, C. A., Hamad, W. Y., & MacLachlan, M. J. (2019). Post-modification of  
446 Cellulose Nanocrystal Aerogels with Thiol-Ene Click Chemistry. *Biomacromolecules*, *20*(7), 2779–2785.  
447 <https://doi.org/10.1021/acs.biomac.9b00533>

448 Abousalman-Rezvani, Z., Eskandari, P., Roghani-Mamaqani, H., & Salami-Kalajahi, M. (2019). Synthesis of coumarin-containing multi-  
449 responsive CNC-grafted and free copolymers with application in nitrate ion removal from aqueous solutions. *Carbohydrate Polymers*,  
450 *225*(June), 115247. <https://doi.org/10.1016/j.carbpol.2019.115247>

451 Abraham, E., Kam, D., Nevo, Y., Slattegard, R., Rivkin, A., Lapidot, S., & Shoseyov, O. (2016). Highly Modified Cellulose Nanocrystals and  
452 Formation of Epoxy-Nanocrystalline Cellulose (CNC) Nanocomposites. *ACS Applied Materials and Interfaces*, *8*(41), 28086–28095.  
453 <https://doi.org/10.1021/acsami.6b09852>

454 Alanis, A., Valdés, J. H., María Guadalupe, N. V., Lopez, R., Mendoza, R., Mathew, A. P., Díaz De León, R., & Valencia, L. (2019). Plasma surface-  
455 modification of cellulose nanocrystals: A green alternative towards mechanical reinforcement of ABS. *RSC Advances*, *9*(30), 17417–  
456 17424. <https://doi.org/10.1039/c9ra02451d>

- 457 Anpilova, A. Y., Mastalygina, E. E., Khrameeva, N. P., & Popov, A. A. (2020). Methods for Cellulose Modification in the Development of  
458 Polymeric Composite Materials (Review). *Russian Journal of Physical Chemistry B*, 14(1), 176–182.  
459 <https://doi.org/10.1134/S1990793120010029>
- 460 Anžlovar, A., Huskić, M., & Žagar, E. (2016). Modification of nanocrystalline cellulose for application as a reinforcing nanofiller in PMMA  
461 composites. *Cellulose*, 23(1), 505–518. <https://doi.org/10.1007/s10570-015-0786-9>
- 462 Arfin, T. (2020). Cellulose and hydrogel matrices for environmental applications. In *Sustainable Nanocellulose and Nanohydrogels from*  
463 *Natural Sources*. INC. <https://doi.org/10.1016/b978-0-12-816789-2.00012-2>
- 464 Arredondo, J., Jessop, P. G., Champagne, P., Bouchard, J., & Cunningham, M. F. (2017). Synthesis of CO<sub>2</sub>-responsive cellulose nanocrystals by  
465 surface-initiated Cu(0)-mediated polymerisation. *Green Chemistry*, 19(17), 4141–4152. <https://doi.org/10.1039/c7gc01798g>
- 466 Arredondo, J., Woodcock, N. M., Garcia-Valdez, O., Jessop, P. G., Champagne, P., & Cunningham, M. F. (2020). Surface modification of  
467 cellulose nanocrystals via RAFT polymerization of CO<sub>2</sub>-responsive monomer-tuning hydrophobicity. *Langmuir*, 36(46), 13989–13997.  
468 <https://doi.org/10.1021/acs.langmuir.0c02509>
- 469 Asempour, F., Emadzadeh, D., Matsuura, T., & Kruczek, B. (2018). Synthesis and characterization of novel Cellulose Nanocrystals-based Thin  
470 Film Nanocomposite membranes for reverse osmosis applications. *Desalination*, 439(December 2017), 179–187.  
471 <https://doi.org/10.1016/j.desal.2018.04.009>
- 472 Ávila Ramírez, J. A., Fortunati, E., Kenny, J. M., Torre, L., & Foresti, M. L. (2017). Simple citric acid-catalyzed surface esterification of cellulose  
473 nanocrystals. *Carbohydrate Polymers*, 157, 1358–1364. <https://doi.org/10.1016/j.carbpol.2016.11.008>
- 474 Bai, Langming, Wu, H., Ding, J., Ding, A., Zhang, X., Ren, N., Li, G., & Liang, H. (2020). Cellulose nanocrystal-blended polyethersulfone  
475 membranes for enhanced removal of natural organic matter and alleviation of membrane fouling. *Chemical Engineering Journal*,  
476 382(September 2019), 122919. <https://doi.org/10.1016/j.cej.2019.122919>
- 477 Bai, Liangjiu, Jiang, X., Sun, Z., Pei, Z., Ma, A., Wang, W., Chen, H., Yang, H., Yang, L., & Wei, D. (2019). Self-healing nanocomposite hydrogels  
478 based on modified cellulose nanocrystals by surface-initiated photoinduced electron transfer ATRP. *Cellulose*, 26(9), 5305–5319.  
479 <https://doi.org/10.1007/s10570-019-02449-2>
- 480 Beck, S., Bouchard, J., & Berry, R. (2011). Controlling the reflection wavelength of iridescent solid films of nanocrystalline cellulose.  
481 *Biomacromolecules*, 12(1), 167–172. <https://doi.org/10.1021/bm1010905>
- 482 Belaustegui, Y., Pantò, F., Urbina, L., Corcuera, M. A., Eceiza, A., Palella, A., Triolo, C., & Santangelo, S. (2020). Bacterial-cellulose-derived  
483 carbonaceous electrode materials for water desalination via capacitive method: The crucial role of defect sites. *Desalination*,  
484 492(July), 114596. <https://doi.org/10.1016/j.desal.2020.114596>
- 485 Bendahou, A., Hajlane, A., Dufresne, A., Boufi, S., & Kaddami, H. (2015). Esterification and amidation for grafting long aliphatic chains on to  
486 cellulose nanocrystals: A comparative study. *Research on Chemical Intermediates*, 41(7), 4293–4310.  
487 <https://doi.org/10.1007/s11164-014-1530-z>
- 488 Boujemaoui, A., Cobo Sanchez, C., Engström, J., Bruce, C., Fogelström, L., Carlmark, A., & Malmström, E. (2017). Polycaprolactone  
489 Nanocomposites Reinforced with Cellulose Nanocrystals Surface-Modified via Covalent Grafting or Physisorption: A Comparative  
490 Study. *ACS Applied Materials and Interfaces*, 9(40), 35305–35318. <https://doi.org/10.1021/acsami.7b09009>
- 491 Boujemaoui, A., Mazières, S., Malmström, E., Destarac, M., & Carlmark, A. (2016). SI-RAFT/MADIX polymerization of vinyl acetate on cellulose  
492 nanocrystals for nanocomposite applications. *Polymer*, 99, 240–249. <https://doi.org/10.1016/j.polymer.2016.07.013>
- 493 Bwatanglang, I. B., Musa, Y., & Yusof, N. A. (2020). Market analysis and commercially available cellulose and hydrogel-based composites for  
494 sustainability, clean environment, and human health. *Sustainable Nanocellulose and Nanohydrogels from Natural Sources*, 65–79.  
495 <https://doi.org/10.1016/b978-0-12-816789-2.00003-1>
- 496 Carlmark, A., Larsson, E., & Malmström, E. (2012). Grafting of cellulose by ring-opening polymerisation - A review. *European Polymer Journal*,  
497 48(10), 1646–1659. <https://doi.org/10.1016/j.eurpolymj.2012.06.013>
- 498 Carlsson, L., Ingverud, T., Blomberg, H., Carlmark, A., Larsson, P. T., & Malmström, E. (2015). Surface characteristics of cellulose nanoparticles  
499 grafted by surface-initiated ring-opening polymerization of ε-caprolactone. *Cellulose*, 22(2), 1063–1074.  
500 <https://doi.org/10.1007/s10570-014-0510-1>
- 501 Chen, Jianxiang, Wu, D., Tam, K. C., Pan, K., & Zheng, Z. (2017). Effect of surface modification of cellulose nanocrystal on nonisothermal  
502 crystallization of poly(β-hydroxybutyrate) composites. *Carbohydrate Polymers*, 157, 1821–1829.  
503 <https://doi.org/10.1016/j.carbpol.2016.11.071>
- 504 Chen, Junyu, Mao, L., Qi, H., Xu, D., Huang, H., Liu, M., Wen, Y., Deng, F., Zhang, X., & Wei, Y. (2020). Preparation of fluorescent cellulose  
505 nanocrystal polymer composites with thermo-responsiveness through light-induced ATRP. *Cellulose*, 27(2), 743–753.  
506 <https://doi.org/10.1007/s10570-019-02845-8>
- 507 Chen, Q., Liu, P., Nan, F., Zhou, L., & Zhang, J. (2014). Tuning the iridescence of chiral nematic cellulose nanocrystal films with a vacuum-  
508 assisted self-assembly technique. *Biomacromolecules*, 15(11), 4343–4350. <https://doi.org/10.1021/bm501355x>



- 509 Chu, Y., Sun, Y., Wu, W., & Xiao, H. (2020). Dispersion Properties of Nanocellulose : A Review. *Carbohydrate Polymers*, 250(July), 116892.  
510 <https://doi.org/10.1016/j.carbpol.2020.116892>
- 511 Cruz-Tato, P., Ortiz-Quiles, E. O., Vega-Figueroa, K., Santiago-Martoral, L., Flynn, M., Díaz-Vázquez, L. M., & Nicolau, E. (2017). Metalized  
512 Nanocellulose Composites as a Feasible Material for Membrane Supports: Design and Applications for Water Treatment.  
513 *Environmental Science and Technology*, 51(8), 4585–4595. <https://doi.org/10.1021/acs.est.6b05955>
- 514 De Castro, D. O., Bras, J., Gandini, A., & Belgacem, N. (2016). Surface grafting of cellulose nanocrystals with natural anti-microbial rosin  
515 mixture using a green process. *Carbohydrate Polymers*, 137, 1–8. <https://doi.org/10.1016/j.carbpol.2015.09.101>
- 516 De Morais Zanata, D., Battirola, L. C., & Gonçalves, M. do C. (2018). Chemically crosslinked aerogels based on cellulose nanocrystals and  
517 polysilsesquioxane. *Cellulose*, 25(12), 7225–7238. <https://doi.org/10.1007/s10570-018-2090-y>
- 518 Dey, D., Dharini, V., Selvam, S. P., Sadiku, E. R., Kumar, M. M., Jayaramudu, J., & Gupta, U. N. (2021). Physical, antifungal, and biodegradable  
519 properties of cellulose nanocrystals and chitosan nanoparticles for food packaging application. *Materials Today: Proceedings*, 38,  
520 860–869. <https://doi.org/10.1016/j.matpr.2020.04.885>
- 521 Dong, Y. D., Zhang, H., Zhong, G. J., Yao, G., & Lai, B. (2021). Cellulose/carbon Composites and their Applications in Water Treatment – a  
522 Review. *Chemical Engineering Journal*, 405(July 2020), 126980. <https://doi.org/10.1016/j.cej.2020.126980>
- 523 Du, X., Zhang, Z., Liu, W., & Deng, Y. (2017). Nanocellulose-based conductive materials and their emerging applications in energy devices - A  
524 review. *Nano Energy*, 35(January), 299–320. <https://doi.org/10.1016/j.nanoen.2017.04.001>
- 525 Dugan, J. M., Gough, J. E., & Eichhorn, S. J. (2010). Directing the morphology and differentiation of skeletal muscle cells using oriented  
526 cellulose nanowhiskers. *Biomacromolecules*, 11(9), 2498–2504. <https://doi.org/10.1021/bm100684k>
- 527 Dumanli, A. G., Kamita, G., Landman, J., Van der Kooji, H., Glover, B., Baumberg, J. J., Steiner, U., & Vignolini, S. (2014). *Controlled, Bio-inspired*  
528 *Self-Assembly of Cellulose-Based Chiral Reflectors* (pp. 646–650).
- 529 Dupont, H., Laurichesse, E., Héroguez, V., & Schmitt, V. (2021). Green Hydrophilic Capsules from Cellulose Nanocrystal-Stabilized Pickering  
530 Emulsion Polymerization: Morphology Control and Spongelike Behavior. *Biomacromolecules*.  
531 <https://doi.org/10.1021/acs.biomac.1c00581>
- 532 El-nahrawy, A. M., Abou, A. B., Khattab, A., & Haroun, A. (2020). *Development of electrically conductive nanocomposites from cellulose*  
533 *nanowhiskers , polypyrrole and silver nanoparticles assisted with Nickel ( III ) oxide nanoparticles*. 149(January).  
534 <https://doi.org/10.1016/j.reactfunctpolym.2020.104533>
- 535 Emam, H. E., & Shaheen, T. I. (2019). Investigation into the Role of Surface Modification of Cellulose Nanocrystals with Succinic Anhydride in  
536 Dye Removal. *Journal of Polymers and the Environment*, 27(11), 2419–2427. <https://doi.org/10.1007/s10924-019-01533-9>
- 537 Eskandari, P., Roghani-Mamaqani, H., Salami-Kalajahi, M., & Abousalman-Rezvani, Z. (2020). Modification of cellulose nanocrystal with dual  
538 temperature- and CO<sub>2</sub>-responsive block copolymers for ion adsorption applications. *Journal of Molecular Liquids*, 310, 113234.  
539 <https://doi.org/10.1016/j.molliq.2020.113234>
- 540 Espino-Pérez, E., Domenek, S., Belgacem, N., Sillard, C., & Bras, J. (2014). Green process for chemical functionalization of nanocellulose with  
541 carboxylic acids. *Biomacromolecules*, 15(12), 4551–4560. <https://doi.org/10.1021/bm5013458>
- 542 Fang, Z., Hou, G., Chen, C., & Hu, L. (2019a). Nanocellulose-based films and their emerging applications. *Current Opinion in Solid State and*  
543 *Materials Science*, 23(4), 100764. <https://doi.org/10.1016/j.cossms.2019.07.003>
- 544 Fang, Z., Hou, G., Chen, C., & Hu, L. (2019b). Nanocellulose-based films and their emerging applications. *Current Opinion in Solid State and*  
545 *Materials Science*, 23(4), 100764. <https://doi.org/10.1016/j.cossms.2019.07.003>
- 546 Filpponen, I. (2014). *Chapter 3: Click Chemistry in Cellulose Functionalization*.
- 547 Fleet, R., McLeary, J. B., Grumel, V., Weber, W. G., Matahwa, H., & Sanderson, R. D. (2008). RAFT mediated polysaccharide copolymers.  
548 *European Polymer Journal*, 44(9), 2899–2911. <https://doi.org/10.1016/j.eurpolymj.2008.06.042>
- 549 Frka-Petescic, B., Guidetti, G., Kamita, G., & Vignolini, S. (2017). Controlling the Photonic Properties of Cholesteric Cellulose Nanocrystal Films  
550 with Magnets. *Advanced Materials*, 29(32), 1–7. <https://doi.org/10.1002/adma.201701469>
- 551 Fumagalli, M., Sanchez, F., Boisseau, S. M., & Heux, L. (2013). Gas-phase esterification of cellulose nanocrystal aerogels for colloidal dispersion  
552 in apolar solvents. *Soft Matter*, 9(47), 11309–11317. <https://doi.org/10.1039/c3sm52062e>
- 553 Garcia-Valdez, O., Champagne, P., & Cunningham, M. F. (2018). Graft modification of natural polysaccharides via reversible deactivation  
554 radical polymerization. *Progress in Polymer Science*, 76, 151–173. <https://doi.org/10.1016/j.progpolymsci.2017.08.001>
- 555 Gauche, C., & Felisberti, M. I. (2019). Colloidal Behavior of Cellulose Nanocrystals Grafted with Poly(2-alkyl-2-oxazoline)s. *ACS Omega*, 4(7),  
556 11893–11905. <https://doi.org/10.1021/acsomega.9b01269>
- 557 Ge, W., Zhao, B., Li, L., Nie, K., & Zheng, S. (2021). Nanocomposites of polyhydroxyurethane with nanocrystalline cellulose: Synthesis,

- 558 thermomechanical and reprocessing properties. *European Polymer Journal*, 149(October 2020), 110287.  
559 <https://doi.org/10.1016/j.eurpolymj.2021.110287>
- 560 Glasing, J., Bouchard, J., Jessop, P. G., Champagne, P., & Cunningham, M. F. (2017). Grafting well-defined CO<sub>2</sub>-responsive polymers to  
561 cellulose nanocrystals via nitroxide-mediated polymerisation: Effect of graft density and molecular weight on dispersion behaviour.  
562 *Polymer Chemistry*, 8(38), 6000–6012. <https://doi.org/10.1039/c7py01258f>
- 563 Goffin, A. L., Raquez, J. M., Duquesne, E., Siqueira, G., Habibi, Y., Dufresne, A., & Dubois, P. (2011). From interfacial ring-opening  
564 polymerization to melt processing of cellulose nanowhisker-filled polylactide-based nanocomposites. *Biomacromolecules*, 12(7),  
565 2456–2465. <https://doi.org/10.1021/bm200581h>
- 566 Gopakumar, D. A., Arumughan, V., Pasquini, D., Leu, S. Y., Abdul Khalil, H. P. S., & Thomas, S. (2018). Nanocellulose-Based Membranes for  
567 Water Purification. In *Nanoscale Materials in Water Purification*. Elsevier Inc. <https://doi.org/10.1016/B978-0-12-813926-4.00004-5>
- 568 Grishkewich, N., Akhlaghi, S. P., Zhaoling, Y., Berry, R., & Tam, K. C. (2016). Cellulose nanocrystal-poly(oligo(ethylene glycol) methacrylate)  
569 brushes with tunable LCSTs. *Carbohydrate Polymers*, 144, 215–222. <https://doi.org/10.1016/j.carbpol.2016.02.044>
- 570 Gupta, A. D., Pandey, S., Jaiswal, V. K., Bhadauria, V., & Singh, H. (2019). Simultaneous oxidation and esterification of cellulose for use in  
571 treatment of water containing Cu(II) ions. *Carbohydrate Polymers*, 222(June), 114964. <https://doi.org/10.1016/j.carbpol.2019.06.003>
- 572 Habibi, Y., Aouadi, S., Raquez, J. M., & Dubois, P. (2013). Effects of interfacial stereocomplexation in cellulose nanocrystal-filled polylactide  
573 nanocomposites. *Cellulose*, 20(6), 2877–2885. <https://doi.org/10.1007/s10570-013-0058-5>
- 574 Hamad, W. (2002). Cellulosic Materials. In *Cellulosic Materials*. <https://doi.org/10.1007/978-1-4615-0825-0>
- 575 Han, S. (2019). *Thermoelectric polymer-cellulose composite aerogels* (Issue 2028).
- 576 Haqani, M., Roghani-Mamaqani, H., & Salami-Kalajahi, M. (2017). Synthesis of dual-sensitive nanocrystalline cellulose-grafted block  
577 copolymers of N-isopropylacrylamide and acrylic acid by reversible addition-fragmentation chain transfer polymerization. *Cellulose*,  
578 24(5), 2241–2254. <https://doi.org/10.1007/s10570-017-1249-2>
- 579 Hoang, M. T., Pham, T. D., Verheyen, D., Nguyen, M. K., Pham, T. T., Zhu, J., & Van der Bruggen, B. (2020). Fabrication of thin film  
580 nanocomposite nanofiltration membrane incorporated with cellulose nanocrystals for removal of Cu(II) and Pb(II). *Chemical*  
581 *Engineering Science*, 228, 115998. <https://doi.org/10.1016/j.ces.2020.115998>
- 582 Hu, H., Hou, X. J., Wang, X. C., Nie, J. J., Cai, Q., & Xu, F. J. (2016). Gold nanoparticle-conjugated heterogeneous polymer brush-wrapped  
583 cellulose nanocrystals prepared by combining different controllable polymerization techniques for theranostic applications. *Polymer*  
584 *Chemistry*, 7(18), 3107–3116. <https://doi.org/10.1039/c6py00251j>
- 585 Huang, J. L., Li, C. J., & Gray, D. G. (2014). Functionalization of cellulose nanocrystal films via “thiol-ene” click reaction. *RSC Advances*, 4(14),  
586 6965–6969. <https://doi.org/10.1039/c3ra47041e>
- 587 Huang, S., Wu, M. B., Zhu, C. Y., Ma, M. Q., Yang, J., Wu, J., & Xu, Z. K. (2019). Polyamide Nanofiltration Membranes Incorporated with  
588 Cellulose Nanocrystals for Enhanced Water Flux and Chlorine Resistance. *ACS Sustainable Chemistry and Engineering*, 7(14), 12315–  
589 12322. <https://doi.org/10.1021/acssuschemeng.9b01651>
- 590 Huang, Y., Chen, G., Liang, Q., Yang, Z., & Shen, H. (2020). Multifunctional cellulose nanocrystal structural colored film with good flexibility  
591 and water-resistance. *International Journal of Biological Macromolecules*, 149, 819–825.  
592 <https://doi.org/10.1016/j.ijbiomac.2020.01.247>
- 593 Jackson, J. C., Camargos, C. H. M., Noronha, V. T., Paula, A. J., Rezende, C. A., & Faria, A. F. (2021). Sustainable Cellulose Nanocrystals for  
594 Improved Anti-microbial Properties of Thin Film Composite Membranes. *ACS Sustainable Chemistry and Engineering*, 9(19), 6534–  
595 6540. <https://doi.org/10.1021/acssuschemeng.1c02389>
- 596 Jeun, J.-P., Lee, Y., Kang, P.-H., & Lee, D.-Y. (2019). Surface Modification for the Hydrophobization of Cellulose Nanocrystals Using Radiation-  
597 Induced Grafting. *Journal of Nanoscience and Nanotechnology*, 19(10), 6303–6308. <https://doi.org/10.1166/jnn.2019.17033>
- 598 Jonoobi, M., Ashori, A., & Siracusa, V. (2019). Characterization and properties of polyethersulfone/ modified cellulose nanocrystals  
599 nanocomposite membranes. *Polymer Testing*, 76(February), 333–339. <https://doi.org/10.1016/j.polymertesting.2019.03.039>
- 600 Karim, Z., Hakalahti, M., Tammelin, T., & Mathew, A. P. (2017). In situ TEMPO surface functionalization of nanocellulose membranes for  
601 enhanced adsorption of metal ions from aqueous medium. *RSC Advances*, 7(9), 5232–5241. <https://doi.org/10.1039/c6ra25707k>
- 602 Karim, Z., Mathew, A. P., Grahn, M., Mouzon, J., & Oksman, K. (2014). Nanoporous membranes with cellulose nanocrystals as functional  
603 entity in chitosan: Removal of dyes from water. *Carbohydrate Polymers*, 112, 668–676.  
604 <https://doi.org/10.1016/j.carbpol.2014.06.048>
- 605 Kashani Rahimi, S., & Otaigbe, J. U. (2016). The role of particle surface functionality and microstructure development in isothermal and non-  
606 isothermal crystallization behavior of polyamide 6/cellulose nanocrystals nanocomposites. *Polymer*, 107, 316–331.  
607 <https://doi.org/10.1016/j.polymer.2016.11.023>

- 608 Kausar, A. (2020). Nanocellulose in polymer nanocomposite. In *Sustainable Nanocellulose and Nanohydrogels from Natural Sources*. INC.  
609 <https://doi.org/10.1016/b978-0-12-816789-2.00017-1>
- 610 Kedzior, S. A., Kiriakou, M., Niinivaara, E., Dubé, M. A., Fraschini, C., Berry, R. M., & Cranston, E. D. (2018). Incorporating Cellulose Nanocrystals  
611 into the Core of Polymer Latex Particles via Polymer Grafting. *ACS Macro Letters*, 7(8), 990–996.  
612 <https://doi.org/10.1021/acsmacrolett.8b00334>
- 613 Kedzior, S. A., Zoppe, J. O., Berry, R. M., & Cranston, E. D. (2019). Recent advances and an industrial perspective of cellulose nanocrystal  
614 functionalization through polymer grafting. *Current Opinion in Solid State and Materials Science*, 23(2), 74–91.  
615 <https://doi.org/10.1016/j.cossms.2018.11.005>
- 616 Khanjanzadeh, H., Behrooz, R., Bahramifar, N., Gindl-Altmutter, W., Bacher, M., Edler, M., & Griesser, T. (2018). Surface chemical  
617 functionalization of cellulose nanocrystals by 3-aminopropyltriethoxysilane. *International Journal of Biological Macromolecules*, 106,  
618 1288–1296. <https://doi.org/10.1016/j.ijbiomac.2017.08.136>
- 619 Kim, H., Park, J., Minn, K. S., Youn, J. R., & Song, Y. S. (2020). Eco-Friendly Nanocellulose Embedded Polymer Composite Foam for Flame  
620 Retardancy Improvement. *Macromolecular Research*, 28(2), 165–171. <https://doi.org/10.1007/s13233-020-8020-5>
- 621 Kiriakou, M. V., Berry, R. M., Hoare, T., & Cranston, E. D. (2021). *E f f e c t of Reaction Media on Grafting Hydrophobic Polymers from Cellulose*  
622 *Nanocrystals via Surface-Initiated Atom-Transfer Radical Polymerization*. <https://doi.org/10.1021/acs.biomac.1c00692>
- 623 Kolb, H. C., Finn, M. G., & Sharpless, K. B. (2001). Click Chemistry: Diverse Chemical Function from a Few Good Reactions. *Angewandte Chemie*  
624 *- International Edition*, 40(11), 2004–2021. [https://doi.org/10.1002/1521-3773\(20010601\)40:11<2004::AID-ANIE2004>3.0.CO;2-5](https://doi.org/10.1002/1521-3773(20010601)40:11<2004::AID-ANIE2004>3.0.CO;2-5)
- 625 Kulandaivalu, S., & Sulaiman, Y. (2020). Rational design of layer-by-layer assembled polypyrrole-based nanocomposite film for high-  
626 performance supercapacitor. *Journal of Materials Science: Materials in Electronics*, 31(6), 4882–4894.  
627 <https://doi.org/10.1007/s10854-020-03051-0>
- 628 Kulandaivalu, S., & Yusran, S. (2019). Recent Advances in Layer-by-Layer Assembled Conducting Polymer Based Composites for  
629 Supercapacitors. *Energies*, 12, 2107.
- 630 Lagerwall, J. P. F., Schütz, C., Salajkova, M., Noh, J., Park, J. H., Scalia, G., & Bergström, L. (2014). Cellulose nanocrystal-based materials: From  
631 liquid crystal self-assembly and glass formation to multifunctional thin films. *NPG Asia Materials*, 6(1), 1–12.  
632 <https://doi.org/10.1038/am.2013.69>
- 633 Leszczyńska, A., Radzik, P., Szefer, E., Mičušík, M., Omastová, M., & Pielichowski, K. (2019). Surface modification of cellulose nanocrystals  
634 with succinic anhydride. *Polymers*, 11(5). <https://doi.org/10.3390/polym11050866>
- 635 Li, Hong, Zhou, J., Zhao, J., Li, Y., & Lu, K. (2020). Synthesis of cellulose nanocrystals-armored fluorinated polyacrylate latexes via Pickering  
636 emulsion polymerization and their film properties. *Colloids and Surfaces B: Biointerfaces*, 192(April), 111071.  
637 <https://doi.org/10.1016/j.colsurfb.2020.111071>
- 638 Li, Hui, Shi, H., He, Y., Fei, X., & Peng, L. (2020). Preparation and characterization of carboxymethyl cellulose-based composite films reinforced  
639 by cellulose nanocrystals derived from pea hull waste for food packaging applications. *International Journal of Biological*  
640 *Macromolecules*, 164, 4104–4112. <https://doi.org/10.1016/j.ijbiomac.2020.09.010>
- 641 Lin, N., Gèze, A., Wouessidjewe, D., Huang, J., & Dufresne, A. (2016). Biocompatible Double-Membrane Hydrogels from Cationic Cellulose  
642 Nanocrystals and Anionic Alginate as Complexing Drugs Codelivery. *ACS Applied Materials and Interfaces*, 8(11), 6880–6889.  
643 <https://doi.org/10.1021/acsmami.6b00555>
- 644 Liu, J., Liu, D., Liu, S., Li, Z., Wei, X., Lin, S., & Guo, M. (2020). Preparation and Characterization of Sulfated Cellulose Nanocrystalline and its  
645 Composite Membrane for Removal of Tetracycline Hydrochloride in Water. *Energy and Environmental Materials*, 3(2), 209–215.  
646 <https://doi.org/10.1002/eem2.12055>
- 647 Liu, S., Chen, Y., Liu, C., Gan, L., Ma, X., & Huang, J. (2019). Polydopamine-coated cellulose nanocrystals as an active ingredient in poly(vinyl  
648 alcohol) films towards intensifying packaging application potential. *Cellulose*, 26(18), 9599–9612. <https://doi.org/10.1007/s10570-019-02749-7>
- 650 Liu, T., Ding, E., & Xue, F. (2017). Polyacrylamide and poly(N,N-dimethylacrylamide) grafted cellulose nanocrystals as efficient flocculants for  
651 kaolin suspension. *International Journal of Biological Macromolecules*, 103, 1107–1112.  
652 <https://doi.org/10.1016/j.ijbiomac.2017.05.098>
- 653 Liu, T., Ding, E., & Xue, F. (2018). Grafting poly(N,N-dimethylacrylamide) from cellulose nanocrystals by the macro-RAFT agent-assisted  
654 strategy. *Cellulose*, 25(3), 1705–1714. <https://doi.org/10.1007/s10570-018-1685-7>
- 655 Liu, T., Xue, F., & Ding, E. (2016). Cellulose nanocrystals grafted with polyacrylamide assisted by macromolecular RAFT agents. *Cellulose*,  
656 23(6), 3717–3735. <https://doi.org/10.1007/s10570-016-1083-y>
- 657 Lizundia, E., Fortunati, E., Dominici, F., Vilas, J. L., León, L. M., Armentano, I., Torre, L., & Kenny, J. M. (2016). PLLA-grafted cellulose  
658 nanocrystals: Role of the CNC content and grafting on the PLA bionanocomposite film properties. *Carbohydrate Polymers*, 142, 105–  
659 113. <https://doi.org/10.1016/j.carbpol.2016.01.041>

- 660 Miao, C., & Hamad, W. Y. (2016). In-situ polymerized cellulose nanocrystals (CNC)—poly(L-lactide) (PLLA) nanomaterials and applications in  
661 nanocomposite processing. *Carbohydrate Polymers*, 153, 549–558. <https://doi.org/10.1016/j.carbpol.2016.08.012>
- 662 Mishra, V., & Kumar, R. (2012). Living Radical Polymerization: a Review. *Journal of Scientific Research Banaras Hindu University*, 56, 141–176.
- 663 Moad, G., Rizzardo, E., & Thang, S. H. (2013). RAFT polymerization and some of its applications. *Chemistry - An Asian Journal*, 8(8), 1634–  
664 1644. <https://doi.org/10.1002/asia.201300262>
- 665 Mohamed, M. A., Abd Mutalib, M., Mohd Hir, Z. A., M. Zain, M. F., Mohamad, A. B., Jeffery Minggu, L., Awang, N. A., & W. Salleh, W. N.  
666 (2017). An overview on cellulose-based material in tailoring bio-hybrid nanostructured photocatalysts for water treatment and  
667 renewable energy applications. *International Journal of Biological Macromolecules*, 103, 1232–1256.  
668 <https://doi.org/10.1016/j.ijbiomac.2017.05.181>
- 669 Morandi, G., Heath, L., & Thielemans, W. (2009). Cellulose nanocrystals grafted with polystyrene chains through Surface-Initiated Atom  
670 Transfer Radical Polymerization (SI-ATRP). *Langmuir*, 25(14), 8280–8286. <https://doi.org/10.1021/la900452a>
- 671 Morits, M., Hynninen, V., Nonappa, Niederberger, A., Ikkala, O., Gröschel, A. H., & Müllner, M. (2018). Polymer brush guided templating on  
672 well-defined rod-like cellulose nanocrystals. *Polymer Chemistry*, 9(13), 1650–1657. <https://doi.org/10.1039/c7py01814b>
- 673 Movagharnegad, N., Najafi Moghadam, P., Nikoo, A., & Shokri, Z. (2018). Modification of Magnetite Cellulose Nanoparticles via Click Reaction  
674 for use in Controlled Drug Delivery. *Polymer - Plastics Technology and Engineering*, 57(18), 1915–1922.  
675 <https://doi.org/10.1080/03602559.2018.1447127>
- 676 Muiruri, J. K., Liu, S., Teo, W. S., Kong, J., & He, C. (2017). Highly Biodegradable and Tough Polylactic Acid-Cellulose Nanocrystal Composite.  
677 *ACS Sustainable Chemistry and Engineering*, 5(5), 3929–3937. <https://doi.org/10.1021/acssuschemeng.6b03123>
- 678 Naseri, N., Mathew, A. P., Girandon, L., Fröhlich, M., & Oksman, K. (2015). Porous electrospun nanocomposite mats based on chitosan–  
679 cellulose nanocrystals for wound dressing: effect of surface characteristics of nanocrystals. *Cellulose*, 22(1), 521–534.  
680 <https://doi.org/10.1007/s10570-014-0493-y>
- 681 Nechyporchuk, O., Belgacem, M. N., & Bras, J. (2016). Production of cellulose nanofibrils : A review of recent advances. *Industrial Crops &*  
682 *Products*, 93, 2–25. <https://doi.org/10.1016/j.indcrop.2016.02.016>
- 683 Nepomuceno, N. C., Seixas, A. A. A., Medeiros, E. S., & Mélo, T. J. A. (2021). Evaluation of conductivity of nanostructured polyaniline/cellulose  
684 nanocrystals (PANI/CNC) obtained via in situ polymerization. *Journal of Solid State Chemistry*, 302(May).  
685 <https://doi.org/10.1016/j.jssc.2021.122372>
- 686 Nuyken, O., & Pask, S. D. (2013). Ring-opening polymerization—An introductory review. *Polymers*, 5(2), 361–403.  
687 <https://doi.org/10.3390/polym5020361>
- 688 Oberlintner, A., Likozar, B., & Novak, U. (2021). Hydrophobic functionalization reactions of structured cellulose nanomaterials: Mechanisms,  
689 kinetics and in silico multi-scale models. *Carbohydrate Polymers*, 259(January). <https://doi.org/10.1016/j.carbpol.2021.117742>
- 690 Okada, M. (2002). Chemical syntheses of biodegradable polymers. *Progress in Polymer Science (Oxford)*, 27(1), 87–133.  
691 [https://doi.org/10.1016/S0079-6700\(01\)00039-9](https://doi.org/10.1016/S0079-6700(01)00039-9)
- 692 ONU. (2019). World population prospects 2019. In *Department of Economic and Social Affairs. World Population Prospects 2019*. (Issue 141).  
693 <http://www.ncbi.nlm.nih.gov/pubmed/12283219>
- 694 Pal, N., Banerjee, S., Roy, P., & Pal, K. (2019). Reduced graphene oxide and PEG-grafted TEMPO-oxidized cellulose nanocrystal reinforced  
695 poly-lactic acid nanocomposite film for biomedical application. *Materials Science and Engineering C*, 104(April), 109956.  
696 <https://doi.org/10.1016/j.msec.2019.109956>
- 697 Parker, R. M., Guidetti, G., Williams, C. A., Zhao, T., Narkevicius, A., Vignolini, S., & Frka-Petesic, B. (2018). The Self-Assembly of Cellulose  
698 Nanocrystals: Hierarchical Design of Visual Appearance. *Advanced Materials*, 30(19). <https://doi.org/10.1002/adma.201704477>
- 699 Phanthong, P., Reubroycharoen, P., Hao, X., Xu, G., Abudula, A., & Guan, G. (2018). Nanocellulose: Extraction and application. *Carbon*  
700 *Resources Conversion*, 1(1), 32–43. <https://doi.org/10.1016/j.crcon.2018.05.004>
- 701 Prathapan, R., McLiesh, H., Garnier, G., & Tabor, R. F. (2018). Surface engineering of transparent cellulose nanocrystal coatings for biomedical  
702 applications. *ACS Applied Bio Materials*, 1(3), 728–737. <https://doi.org/10.1021/acsbam.8b00193>
- 703 Qin, L., Gao, H., Xiong, S., Jia, Y., & Ren, L. (2020). Preparation of collagen/cellulose nanocrystals composite films and their potential  
704 applications in corneal repair. *Journal of Materials Science: Materials in Medicine*, 31(6). <https://doi.org/10.1007/s10856-020-06386-6>  
705
- 706 Qin, X., Ge, W., Mei, H., Li, L., & Zheng, S. (2021). Toughness improvement of epoxy thermosets with cellulose nanocrystals. *Polymer*  
707 *International, January*. <https://doi.org/10.1002/pi.6260>
- 708 Rahimi, S. K., & Otaibge, J. U. (2016). Polyamide 6 Nanocomposites Incorporating Cellulose Nanocrystals Prepared by In-Situ Ring Opening  
709 Polymerization: Viscoelasticity, Creep Behavior, and Melt Rheological Properties. *Polymer Engineering and Science*, 56(9), 1045–1060.

- 710 <https://doi.org/10.1002/pen>
- 711 Revin, V., Liyaskina, E., Nazarkina, M., Bogatyreva, A., & Shchankin, M. (2018). Cost-effective production of bacterial cellulose using acidic  
712 food industry by-products. *Brazilian Journal of Microbiology*, 49, 151–159. <https://doi.org/10.1016/j.bjm.2017.12.012>
- 713 Roeder, R. D., Garcia-Valdez, O., Whitney, R. A., Champagne, P., & Cunningham, M. F. (2016). Graft modification of cellulose nanocrystals:  
714 Via nitroxide-mediated polymerisation. *Polymer Chemistry*, 7(41), 6383–6390. <https://doi.org/10.1039/c6py01515h>
- 715 Rosilo, H., McKee, J. R., Kontturi, E., Koho, T., Hytönen, V. P., Ikkala, O., & Kostianen, M. A. (2014). Cationic polymer brush-modified cellulose  
716 nanocrystals for high-affinity virus binding. *Nanoscale*, 6(20), 11871–11881. <https://doi.org/10.1039/c4nr03584d>
- 717 Roy, D., Semsarilar, M., Guthrie, J. T., & Perrier, S. (2009). Cellulose modification by polymer grafting: A review. *Chemical Society Reviews*,  
718 38(7), 2046–2064. <https://doi.org/10.1039/b808639g>
- 719 Salmieri, S., Islam, F., Khan, R. A., Hossain, F. M., Ibrahim, H. M. M., Miao, C., Hamad, W. Y., & Lacroix, M. (2014). Anti-microbial  
720 nanocomposite films made of poly(lactic acid)-cellulose nanocrystals (PLA-CNC) in food applications: Part A-effect of nisin release on  
721 the inactivation of *Listeria monocytogenes* in ham. *Cellulose*, 21(3), 1837–1850. <https://doi.org/10.1007/s10570-014-0230-6>
- 722 Sarazin, Y., & Carpentier, J. F. (2015). Discrete Cationic Complexes for Ring-Opening Polymerization Catalysis of Cyclic Esters and Epoxides.  
723 *Chemical Reviews*, 115(9), 3564–3614. <https://doi.org/10.1021/acs.chemrev.5b00033>
- 724 Seabra, A. B., Bernardes, J. S., Fávoro, W. J., Paula, A. J., & Durán, N. (2018). Cellulose nanocrystals as carriers in medicine and their toxicities:  
725 A review. *Carbohydrate Polymers*, 181(October 2017), 514–527. <https://doi.org/10.1016/j.carbpol.2017.12.014>
- 726 Seibe, G., Ham-Pichavant, F., & Pecastaings, G. (2013). Dispersibility and emulsion-stabilizing effect of cellulose nanowhiskers esterified by  
727 vinyl acetate and vinyl cinnamate. *Biomacromolecules*, 14(8), 2937–2944. <https://doi.org/10.1021/bm400854n>
- 728 Semsarilar, M., & Perrier, S. (2010). “Green” reversible addition-fragmentation chain-transfer (RAFT) polymerization. *Nature Publishing  
729 Group*, 2(10), 811–820. <https://doi.org/10.1038/nchem.853>
- 730 Sharma, M., Aguado, R., Murtinho, D., Valente, A. J. M., Mendes De Sousa, A. P., & Ferreira, P. J. T. (2020). A review on cationic starch and  
731 nanocellulose as paper coating components. *International Journal of Biological Macromolecules*, 162, 578–598.  
732 <https://doi.org/10.1016/j.ijbiomac.2020.06.131>
- 733 Shojaeiarani, J., Bajwa, D. S., & Hartman, K. (2019). Esterified cellulose nanocrystals as reinforcement in poly(lactic acid) nanocomposites.  
734 *Cellulose*, 26(4), 2349–2362. <https://doi.org/10.1007/s10570-018-02237-4>
- 735 Shojaeiarani, J., Bajwa, D. S., Stark, N. M., Bergholz, T. M., & Kraft, A. L. (2020). Spin coating method improved the performance characteristics  
736 of films obtained from poly(lactic acid) and cellulose nanocrystals. *Sustainable Materials and Technologies*, 26, e00212.  
737 <https://doi.org/10.1016/j.susmat.2020.e00212>
- 738 Silva, A. C. D., Moura Filho, F., Alves, M. R. A., de Menezes, A. J., & Silva, M. C. (2021). Hybrid organic semiconductors from P3HT and cellulose  
739 nanocrystals modified with 3-thiopheneacetic acid. *Synthetic Metals*, 278(January), 116804.  
740 <https://doi.org/10.1016/j.synthmet.2021.116804>
- 741 Singh, S., Dhakar, G. L., Kapgata, B. P., Maji, P. K., Verma, C., Chhajed, M., Rajkumar, K., & Das, C. (2020). Synthesis and chemical modification  
742 of crystalline nanocellulose to reinforce natural rubber composites. *Polymers for Advanced Technologies*, 31(12), 3059–3069.  
743 <https://doi.org/10.1002/pat.5030>
- 744 Spinella, S., Maiorana, A., Qian, Q., Dawson, N. J., Hepworth, V., McCallum, S. A., Ganesh, M., Singer, K. D., & Gross, R. A. (2016). Concurrent  
745 Cellulose Hydrolysis and Esterification to Prepare a Surface-Modified Cellulose Nanocrystal Decorated with Carboxylic Acid Moieties.  
746 *ACS Sustainable Chemistry and Engineering*, 4(3), 1538–1550. <https://doi.org/10.1021/acssuschemeng.5b01489>
- 747 Sudhakar, Y. N., Selvakumar, M., & Bhat, D. K. (2018). An introduction of Biopolymer Electrolytes. In *Biopolymer Electrolytes*.  
748 <https://doi.org/10.1016/b978-0-12-813447-4.00001-7>
- 749 Tran, A., Boott, C. E., & MacLachlan, M. J. (2020). Understanding the Self-Assembly of Cellulose Nanocrystals—Toward Chiral Photonic  
750 Materials. *Advanced Materials*, 32(41), 1–15. <https://doi.org/10.1002/adma.201905876>
- 751 Tran, A., Hamad, W. Y., & MacLachlan, M. J. (2018). Tactoid Annealing Improves Order in Self-Assembled Cellulose Nanocrystal Films with  
752 Chiral Nematic Structures. *Langmuir*, 34(2), 646–652. <https://doi.org/10.1021/acs.langmuir.7b03920>
- 753 Trinh, B. M., & Mekonnen, T. (2018). Hydrophobic esterification of cellulose nanocrystals for epoxy reinforcement. *Polymer*, 155(May), 64–  
754 74. <https://doi.org/10.1016/j.polymer.2018.08.076>
- 755 Tsang, E. M. W., & Holdcroft, S. (2012). Alternative Proton Exchange Membranes by Chain-Growth Polymerization. In *Polymer Science: A  
756 Comprehensive Reference*, 10 Volume Set (Vol. 10). Elsevier B.V. <https://doi.org/10.1016/B978-0-444-53349-4.00285-5>
- 757 Wågberg, L., & Erlandsson, J. (2021). The Use of Layer-by-Layer Self-Assembly and Nanocellulose to Prepare Advanced Functional Materials.  
758 *Advanced Materials*, 33(28), 1–13. <https://doi.org/10.1002/adma.202001474>

- 759 Wang, H., He, J., Zhang, M., Tam, K. C., & Ni, P. (2015). A new pathway towards polymer modified cellulose nanocrystals via a "grafting onto"  
760 process for drug delivery. *Polymer Chemistry*, 6(23), 4206–4209. <https://doi.org/10.1039/c5py00466g>
- 761 Wang, J. J., Yang, H. C., Wu, M. B., Zhang, X., & Xu, Z. K. (2017). Nanofiltration membranes with cellulose nanocrystals as an interlayer for  
762 unprecedented performance. *Journal of Materials Chemistry A*, 5(31), 16289–16295. <https://doi.org/10.1039/c7ta00501f>
- 763 Wang, S., Wei, C., Gong, Y., Lv, J., Yu, C., & Yu, J. (2016). Cellulose nanofiber-assisted dispersion of cellulose nanocrystals@polyaniline in water  
764 and its conductive films. *RSC Advances*, 6(12), 10168–10174. <https://doi.org/10.1039/c5ra19346j>
- 765 Wang, Wei, Liang, T., Zhang, B., Bai, H., Ma, P., & Dong, W. (2018). Green functionalization of cellulose nanocrystals for application in  
766 reinforced poly(methyl methacrylate) nanocomposites. *Carbohydrate Polymers*, 202(May), 591–599.  
767 <https://doi.org/10.1016/j.carbpol.2018.09.019>
- 768 Wang, Wentao, Wang, F., Zhang, C., Wang, Z., Tang, J., Zeng, X., & Wan, X. (2020). Robust, Reprocessable, and Reconfigurable Cellulose-  
769 Based Multiple Shape Memory Polymer Enabled by Dynamic Metal-Ligand Bonds. *ACS Applied Materials and Interfaces*, 12(22),  
770 25233–25242. <https://doi.org/10.1021/acsami.9b13316>
- 771 Wang, X., Cheng, W., Wang, D., Ni, X., & Han, G. (2019). Electrospun polyvinylidene fluoride-based fibrous nanocomposite membranes  
772 reinforced by cellulose nanocrystals for efficient separation of water-in-oil emulsions. *Journal of Membrane Science*, 575(August  
773 2018), 71–79. <https://doi.org/10.1016/j.memsci.2018.12.057>
- 774 Wei, L., Agarwal, U. P., Hirth, K. C., Matuana, L. M., Sabo, R. C., & Stark, N. M. (2017). Chemical modification of nanocellulose with canola oil  
775 fatty acid methyl ester. *Carbohydrate Polymers*, 169, 108–116. <https://doi.org/10.1016/j.carbpol.2017.04.008>
- 776 Wiley, J., & Sons. (2011). Degree of Substitution. *Encyclopedia of Polymer Science and Technology*, 2, 1–2.  
777 <https://doi.org/10.1002/0471440264.pst445>
- 778 Wohlhauser, S., Delepierre, G., Labet, M., Morandi, G., Thielemans, W., Weder, C., & Zoppe, J. O. (2018). Grafting Polymers from Cellulose  
779 Nanocrystals: Synthesis, Properties, and Applications. *Macromolecules*, 51(16), 6157–6189.  
780 <https://doi.org/10.1021/acs.macromol.8b00733>
- 781 Wu, H., Nagarajan, S., Shu, J., Zhang, T., Zhou, L., Duan, Y., & Zhang, J. (2018). Green and facile surface modification of cellulose nanocrystal  
782 as the route to produce poly(lactic acid) nanocomposites with improved properties. *Carbohydrate Polymers*, 197(February), 204–214.  
783 <https://doi.org/10.1016/j.carbpol.2018.05.087>
- 784 Wu, H., Nagarajan, S., Zhou, L., Duan, Y., & Zhang, J. (2016). Synthesis and characterization of cellulose nanocrystal-graft-poly(D-lactide) and  
785 its nanocomposite with poly(L-lactide). *Polymer*, 103, 365–375. <https://doi.org/10.1016/j.polymer.2016.09.070>
- 786 Wu, M. B., Zhang, C., Pi, J. K., Liu, C., Yang, J., & Xu, Z. K. (2019). Cellulose nanocrystals as anti-oil nanomaterials for separating crude oil from  
787 aqueous emulsions and mixtures. *Journal of Materials Chemistry A*, 7(12), 7033–7041. <https://doi.org/10.1039/c9ta00420c>
- 788 Wu, X., Tang, J., Duan, Y., Yu, A., & Berry, M. (2014). *Conductive cellulose nanocrystals with high cycling stability for supercapacitor  
789 applications*. 19268–19274. <https://doi.org/10.1039/c4ta04929b>
- 790 Xia, T., Yuwen, H., & Lin, N. (2018). Self-bonding sandwiched membranes from PDMS and cellulose nanocrystals by engineering strategy of  
791 layer-by-layer curing. *Composites Science and Technology*, 161(November 2017), 8–15.  
792 <https://doi.org/10.1016/j.compscitech.2018.03.038>
- 793 Xiong, R., Yu, S., Smith, M. J., Zhou, J., Krecker, M., Zhang, L., Nepal, D., Bunning, T. J., & Tsukruk, V. V. (2019). Self-Assembly of Emissive  
794 Nanocellulose/Quantum Dot Nanostructures for Chiral Fluorescent Materials. *ACS Nano*, 13(8), 9074–9081.  
795 <https://doi.org/10.1021/acs.nano.9b03305>
- 796 Xu, C., Chen, W., Gao, H., Xie, X., & Chen, Y. (2020). Cellulose nanocrystal/silver (CNC/Ag) thin-film nanocomposite nanofiltration membranes  
797 with multifunctional properties. *Environmental Science: Nano*, 7(3), 803–816. <https://doi.org/10.1039/c9en01367a>
- 798 Xu, Q., Yi, J., Zhang, X., & Zhang, H. (2008). A novel amphotropic polymer based on cellulose nanocrystals grafted with azo polymers. *European  
799 Polymer Journal*, 44(9), 2830–2837. <https://doi.org/10.1016/j.eurpolymj.2008.06.010>
- 800 Xu, Z., Peng, S., Zhou, G., & Xu, X. (2020). Highly hydrophobic, homogeneous suspension and resin by graft copolymerization modification of  
801 cellulose nanocrystal (Cnc). *Journal of Composites Science*, 4(4), 1–9. <https://doi.org/10.3390/jcs4040186>
- 802 Yadav, M., Liu, Y. K., & Chiu, F. C. (2019). Fabrication of cellulose nanocrystal/silver/alginate bionanocomposite films with enhanced  
803 mechanical and barrier properties for food packaging application. *Nanomaterials*, 9(11). <https://doi.org/10.3390/nano9111523>
- 804 Yao, H., Zhou, J., Li, H., & Zhao, J. (2019). Nanocrystalline cellulose/fluorinated polyacrylate latex via RAFT-mediated surfactant-free emulsion  
805 polymerization and its application as waterborne textile finishing agent. *Journal of Polymer Science, Part A: Polymer Chemistry*, 57(12),  
806 1305–1314. <https://doi.org/10.1002/pola.29390>
- 807 Yi, J., Xu, Q., Zhang, X., & Zhang, H. (2009). Temperature-induced chiral nematic phase changes of suspensions of poly(N,N-  
808 dimethylaminoethyl methacrylate)-grafted cellulose nanocrystals. *Cellulose*, 16(6), 989–997. <https://doi.org/10.1007/s10570-009-9350-9>  
809

- 810 Yuan, W., Wang, C., Lei, S., Chen, J., Lei, S., & Li, Z. (2018). Ultraviolet light-, temperature- and pH-responsive fluorescent sensors based on  
811 cellulose nanocrystals. *Polymer Chemistry*, 9(22), 3098–3107. <https://doi.org/10.1039/c8py00613j>
- 812 Zeimaran, E., Pourshahrestani, S., Kadri, N. A., Kong, D., Shirazi, S. F. S., Naveen, S. V., Murugan, S. S., Kumaravel, T. S., & Salamatnia, B.  
813 (2019). Self-Healing Polyester Urethane Supramolecular Elastomers Reinforced with Cellulose Nanocrystals for Biomedical  
814 Applications. *Macromolecular Bioscience*, 19(10), 1–12. <https://doi.org/10.1002/mabi.201900176>
- 815 Zeinali, E., Haddadi-Asl, V., & Roghani-Mamaqani, H. (2014). Nanocrystalline cellulose grafted random copolymers of N- isopropylacrylamide  
816 and acrylic acid synthesized by RAFT polymerization: Effect of different acrylic acid contents on LCST behavior. *RSC Advances*, 4(59),  
817 31428–31442. <https://doi.org/10.1039/c4ra05442c>
- 818 Zeinali, E., Haddadi-Asl, V., & Roghani-Mamaqani, H. (2018). Synthesis of dual thermo- and pH-sensitive poly(N-isopropylacrylamide-co-  
819 acrylic acid)-grafted cellulose nanocrystals by reversible addition-fragmentation chain transfer polymerization. *Journal of Biomedical  
820 Materials Research - Part A*, 106(1), 231–243. <https://doi.org/10.1002/jbm.a.36230>
- 821 Zhang, X., Zhang, J., Dong, L., Ren, S., Wu, Q., & Lei, T. (2017). Thermoresponsive poly(poly(ethylene glycol) methylacrylate)s grafted cellulose  
822 nanocrystals through SI-ATRP polymerization. *Cellulose*, 24(10), 4189–4203. <https://doi.org/10.1007/s10570-017-1414-7>
- 823 Zhang, Z., Sèbe, G., Wang, X., & Tam, K. C. (2018a). Gold nanoparticles stabilized by poly(4-vinylpyridine) grafted cellulose nanocrystals as  
824 efficient and recyclable catalysts. *Carbohydrate Polymers*, 182(August 2017), 61–68. <https://doi.org/10.1016/j.carbpol.2017.10.094>
- 825 Zhang, Z., Sèbe, G., Wang, X., & Tam, K. C. (2018b). UV-Absorbing Cellulose Nanocrystals as Functional Reinforcing Fillers in Poly(vinyl chloride)  
826 Films. *ACS Applied Nano Materials*, 1(2), 632–641. <https://doi.org/10.1021/acsnm.7b00126>
- 827 Zhang, Z., Tam, K. C., Sèbe, G., & Wang, X. (2018). Convenient characterization of polymers grafted on cellulose nanocrystals via SI-ATRP  
828 without chain cleavage. *Carbohydrate Polymers*, 199(July), 603–609. <https://doi.org/10.1016/j.carbpol.2018.07.060>
- 829 Zhang, Z., Wang, X., Tam, K. C., & Sèbe, G. (2019). A comparative study on grafting polymers from cellulose nanocrystals via surface-initiated  
830 atom transfer radical polymerization ( ATRP ) and activator re-generated by electron transfer ATRP. *Carbohydrate Polymers*,  
831 205(September 2018), 322–329. <https://doi.org/10.1016/j.carbpol.2018.10.050>
- 832 Zhou, J., Li, H., Li, Y., & Li, X. (2021). V-Shaped amphiphilic polymer brushes grafted on cellulose nanocrystals: Synthesis, characterization and  
833 properties. *Journal of Physics and Chemistry of Solids*, 154(March), 110056. <https://doi.org/10.1016/j.jpcs.2021.110056>
- 834 Zhou, J., Li, Y., Li, H., & Yao, H. (2019). Cellulose nanocrystals/fluorinated polyacrylate soap-free emulsion prepared via RAFT-assisted  
835 Pickering emulsion polymerization. *Colloids and Surfaces B: Biointerfaces*, 177(February), 321–328.  
836 <https://doi.org/10.1016/j.colsurfb.2019.02.005>
- 837 Zhou, L., He, H., Li, M. C., Huang, S., Mei, C., & Wu, Q. (2018). Grafting polycaprolactone diol onto cellulose nanocrystals via click chemistry:  
838 Enhancing thermal stability and hydrophobic property. *Carbohydrate Polymers*, 189(January), 331–341.  
839 <https://doi.org/10.1016/j.carbpol.2018.02.039>
- 840 Zhou, L., Zhai, Y. M., Yang, M. B., & Yang, W. (2019). Flexible and Tough Cellulose Nanocrystal/Polycaprolactone Hybrid Aerogel Based on the  
841 Strategy of Macromolecule Crosslinking via Click Chemistry. *ACS Sustainable Chemistry and Engineering*, 7(18), 15617–15627.  
842 <https://doi.org/10.1021/acssuschemeng.9b03640>
- 843 Zhu, C. Y., Zhang, X., & Xu, Z. K. (2021). Polyamide-based membranes consisting of nanocomposite interlayers for high performance  
844 nanofiltration. *Journal of Applied Polymer Science*, 138(9), 1–9. <https://doi.org/10.1002/app.49940>
- 845 Zhu, W., Yao, Y., Zhang, Y., Jiang, H., Wang, Z., Chen, W., & Xue, Y. (2020). Preparation of an Amine-Modified Cellulose Nanocrystal Aerogel  
846 by Chemical Vapor Deposition and Its Application in CO<sub>2</sub>Capture. *Industrial and Engineering Chemistry Research*, 59(38), 16660–  
847 16668. <https://doi.org/10.1021/acs.iecr.0c02687>
- 848 Zoppe, J. O., Dupire, A. V. M., Lachat, T. G. G., Lemal, P., Rodriguez-Lorenzo, L., Petri-Fink, A., Weder, C., & Klok, H. A. (2017). Cellulose  
849 Nanocrystals with Tethered Polymer Chains: Chemically Patchy versus Uniform Decoration. *ACS Macro Letters*, 6(9), 892–897.  
850 <https://doi.org/10.1021/acsmacrolett.7b00383s>

